Mass and Heat Transfer in Vial Freeze-Drying of Pharmaceuticals: Role of the Vial

M. J. PIKAL ˣ, M. L. ROY, and SAROJ SHAH

Received April 25, 1983, from the *Lilly Research Laboratories, Eli Lilly and Company, Indianapolis, IN 46285.* Accepted for publication June 8, 1983.

Abstract □ Flow of water vapor is impeded by three barriers or resistances: resistance of the dried-product layer, resistance of the semistoppered vial, and resistance of the chamber. The relationship between heat flow and temperature difference may be described by a vial heat transfer coefficient which has contributions from three parallel mechanisms: (*a*) direct conduction from the shelf to the vial *via* points of direct contact between the vial and shelf, (*b*) conduction through the vapor between the vial bottom and the shelf, and (*c*) radiative heat transfer. This report describes experimental studies of the resistance of semistoppered vials, the resistance of the chamber, and vial heat transfer coefficients. Mass transfer through the semistoppered vial has significant contributions from both Knudsen- and viscous-flow mechanisms. Stopper and chamber resistances are of the same magnitude and are about a factor of 10 less than the dried product resistance. All three heat transfer mechanisms are significant, the relative contributions depending on both the chamber pressure and the type of vial. Vial heat transfer coefficients are sensitive to the geometry of the vial bottom, and even vials of nominally the same specifications may differ significantly in heat transfer characteristics. Vials from the same lot are relatively uniform in their heat transfer characteristics, the relative standard deviation of the vial heat transfer coefficient being only ~4%. The temperature distribution in the frozen product is adequately described by a constant temperature gradient in the vertical direction and the thermal conductivity of ice.

Keyphrases □ Freeze-drying—vial heat transfer coefficients, measurement of resistance to mass transfer □ Heat transfer coefficients—freeze-drying, experimental measurement, mechanisms

Freeze-drying, or lyophilization, is the process by which the solvent, normally water, is removed from a frozen solution by sublimation. The freeze-drying process may be divided into three stages: freezing, primary drying, and secondary drying. For pharmaceutical products, the solution is normally filled into vials and then stoppers are partially inserted into the vial necks (semistoppered position), such that openings for vapor flow are present. Next, the vials are placed on temperature-controlled shelves in the freeze-drying chamber. After freezing, the chamber is evacuated to the desired pressure, normally in the range of 30–500 μm, and the shelf temperature is increased to provide energy for sublimation of ice during primary drying. Secondary drying, which is removal of water from the solute phase, begins in a local region of the sample when the ice has been removed from that region and normally continues for some time after all of the ice has been removed from the sample.

Due to high equipment costs, there is considerable economic motivation to minimize process times (1) while maintaining a low level of product loss arising from either eutectic melt or collapse (2). Optimization of the primary-drying stage requires a knowledge of the maximum allowable product temperature, which is either the eutectic temperature (for a crystalline solute) or the collapse temperature (for an amorphous solute), and also requires a determination of the optimum shelf temperature and chamber pressure–time profile required to maintain the product temperature slightly lower than the maximum allowable temperature during all of primary drying. In practice, the shelf temperature and chamber pressure–time relationship is often determined by trial and error. Since, in principle, optimization of this relationship is a problem in coupled mass and heat transfer, a better fundamental understanding of mass and heat transfer in primary drying would allow greater efficiency in process development and minimize problems encountered on scaleup to production operations.

Passing from the frozen product to the condenser, the flow of water vapor is impeded by three barriers or resistances: (*a*) resistance of the dried-product layer above the frozen product, which in addition to being product dependent is also dependent on the vial used (both the area of the ice–vapor interface and the thickness of the dried-product layer) (3), (*b*) resistance of the semistoppered vial, and (*c*) resistance in transfer from the drying chamber to the condenser. Heat for sublimation must be transferred to the product on the vial bottom from the surface upon which the vial rests and through the frozen solution to the subliming ice. For purposes of this discussion, it will be assumed that the vials are placed directly on the dryer shelf. The relationship between heat flow and temperature difference may be characterized by a vial heat transfer coefficient which has contributions from three parallel mechanisms for heat flow: direct conduction from the surface to the vial *via* points of direct contact between the vial and the shelf, conduction through the vapor between the vial bottom and the shelf, and by radiation heat transfer.

The resistance of the dried product was the subject of an earlier experimental study from this laboratory (3), while several aspects of heat transfer have been addressed by Nail (4). He demonstrated that, for a system of vials in a metal tray placed on a heated shelf, the sublimation rate increased as the chamber pressure was increased. Theoretical arguments were used to demonstrate that the temperature differences across the frozen product, across the glass at the vial bottom, and across the metal tray bottom are small and, therefore, the largest temperature differences, or thermal resistances, were across the vapor boundaries between surfaces. In this case, there were two vapor boundaries, one between the vial bottom and the tray surface upon which the vials rested, and the other between the tray bottom and the shelf. However, since Nail's methodology did not allow the thermal resistances for the two vapor boundaries to be evaluated separately, vial heat transfer coefficients could not be determined.

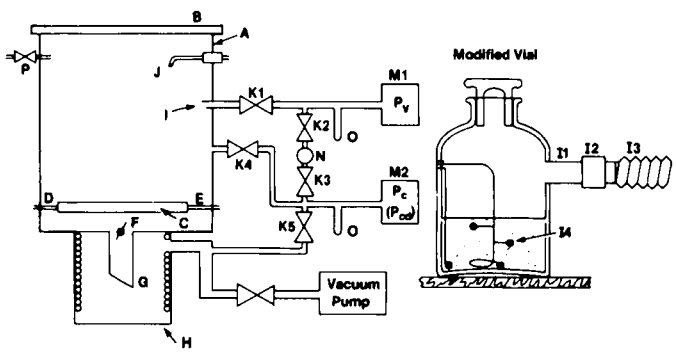

Figure 1—*Schematic of the laboratory freeze-dryer (see text for key).*

0022-3549/84/0900-1224$01.00/0

Table I—Geometric Parameters of Vials

Vial	A_v, cm^2	A_p, cm^2	Neck Finish, mm	Contact o.d., cm	Print Thickness, cm	l_{max}, cm
W5800	4.71	3.80	20	1.90	0.05	0.12
K5800	4.71	3.80	20	1.75	0.12	0.07
W5811	4.71	3.80	20	1.88	0.07	0.04
W5816	6.83	5.71	20	2.24	0.07	0.11
K5816	6.83	5.71	20	2.30[a]	—[a]	0.04
W, K5303	17.2	14.3	28	3.74	0.08	0.22
K5304	8.3	6.72	13	2.60	0.03	0.17

[a] These vials frequently show two concentric prints with the procedure used. The diameter given is the outer diameter of the largest print.

This research describes experimental studies which evaluate: (*a*) mass transfer coefficients (resistances) for several stoppers in the semistoppered configurations, (*b*) resistance of the chamber-to-condenser pathway in a laboratory dryer, and (*c*) vial heat transfer coefficients as a function of chamber pressure for seven types of vials, including examples of both tubing and molded vials. With the aid of a theoretical model for heat transfer, the relative contributions of the three mechanisms of heat flow are examined. Further, since variability in heat transfer coefficients within a given lot of vials is an important consideration in process development, the standard deviation of heat transfer coefficients is determined at selected chamber pressures for six of the seven types of vials studied.

THEORETICAL SECTION

Definition of Mass Transfer Coefficients—Mass transfer is discussed in terms of resistance offered by a given barrier. Resistance, rather than permeability, is used since the total resistance is the sum of component resistances in series. Assuming the usual proportion between flow rate through the barrier and driving force for the process, resistance is defined as the ratio of driving force to flow rate. Since the driving force for both sublimation at the ice-vapor interface and Knudsen flow (3–5)[1] of vapor through the small pores of a dried product is a difference in partial pressures of water (5), the difference between the equilibrium vapor pressure of subliming ice and the partial pressure of water above the dried product is taken as the driving force in the definition of the resistance of the dried product. For vapor flow through the semistoppered vial neck and through the chamber condenser pathway, the driving force is more appropriately taken as a difference in total pressure, to be consistent with the driving force for viscous flow of a fluid (5)[1].

The resistance of the dried-product layer, R_p, is defined by:

$$R_p = (P_0 - x_1^v P_v)/\dot{m} \quad \text{(Eq. 1)}$$

where P_0 is the equilibrium vapor pressure (mm Hg) of the subliming ice, x_1^v is the mole fraction of water vapor in the vial, P_v is the total pressure in the vial (mm Hg), and $\dot{m}$ is the sublimation rate (g/h/vial). As will be shown later, $x_1^v \approx 1$. The normalized product resistance, $\hat{R}_p$, is an area-normalized quantity (independent of product area) given by:

$$\hat{R}_p = A_p R_p \quad \text{(Eq. 2)}$$

where A_p is the geometric cross-sectional area of the product normal to the direction of water vapor flow (computed from the internal diameter of the vial).

The resistance of the semistoppered vial, R_s, is defined by:

$$R_s = (P_v - P_c)/\dot{m} \quad \text{(Eq. 3)}$$

where P_c is the chamber pressure (mm Hg). The resistance of the chamber to condenser pathway, R_c, is defined similarly:

$$R_c = (P_c - P_{cd})/\dot{m}N \quad \text{(Eq. 4)}$$

where N is the number of vials in the dryer and P_{cd} is the pressure in the condenser chamber.

Assuming $x_1^v = 1$, the combination of Eqs. 1–4 yields:

$$\dot{m} = R_T^{-1}(P_0 - P_{cd}) \quad \text{(Eq. 5)}$$

where the total resistance to flow from a given vial to the condenser chamber, R_T, is:

$$R_T = R_p + R_s + NR_c \quad \text{(Eq. 6)}$$

Thus, the contributions to total resistance offered by the dried product, stopper, and chamber are, respectively: R_p, R_s, and NR_c. The quantity NR_c, is a "scaled" chamber resistance and, in effect, is the chamber resistance per vial.

Since the mean free path of water vapor in the dried product is large compared with pore dimensions in the dried product, flow in this region is free molecular or Knudsen flow and the dried-product resistance (R_p) is, therefore, independent of pressure (3, 5). However, the mean free path is smaller than the channels in the stopper and the chamber through which vapor must flow and, hence, the flow mechanism is expected to be predominantly viscous flow with perhaps some contribution from Knudsen flow. Therefore, the stopper and chamber resistances should be pressure dependent and are expected (5) to be of the form:

$$R_i^{-1} = a_0 + a_1\bar{P}_i, \; i = s, c \quad \text{(Eq. 7)}$$

where R_i refers to either R_s or R_c and $\bar{P}_i$ is the mean pressure across the barrier. For example, for $i = s$, $\bar{P}_s = (P_v + P_c)/2$.

The form of Eq. 7 assumes that viscous flow may be described by Poiseuille's law. For viscous flow in short tubes, a correction to Poiseuille's law (5) leads to an additional term in Eq. 7 which is proportional to the product of the sublimation rate and the mean pressure. However, the equations presented by Dushman (5) indicate that the short tube correction is small for both closure resistance and resistance of the laboratory dryer chamber. A preliminary study of closure resistance data (3) suggests that the sublimation rate dependence of the closure resistance is negligible. Thus, although not rigorous, Eq. 7 should serve as a useful first approximation.

Definition of Heat Transfer Coefficients—A heat transfer coefficient is defined as the ratio of the area-normalized heat flow to the temperature difference between heat source and heat sink. For the case of vials resting directly on the freeze-dryer shelf, the vial heat transfer coefficient, K_v, is defined by:

$$\dot{Q} = A_v K_v (T_s - T_b) \quad \text{(Eq. 8)}$$

where $\dot{Q}$ (cal/s) is the heat flow from the shelves to the product in a given vial, A_v is the cross-sectional area of the vial calculated from the vial outer diameter, T_s is the temperature of the shelf surface, and T_b is the temperature of the product at the bottom center of the vial. If the vials are resting on a tray bottom, the temperature T_s refers to the tray surface temperature. Equation 8 assumes the surface above the vials is also at T_s and further assumes the normal situation of a small temperature differential between subliming ice and ice at the vial bottom.

The vial heat transfer coefficient may be expressed as the sum of three terms:

$$K_v = K_c + K_r + K_g \quad \text{(Eq. 9)}$$

[1] When the mean free path is large compared with the dimensions of the pores or tubes constituting the physical system responsible for resistance to flow, as is the case with flow through a dried product (3), collisions of water molecules with the pore or tube walls are responsible for resistance to flow, and the flow mechanism is said to be free molecular flow or Knudsen flow (5). Here, the driving force is the difference in partial pressure of the flowing gas under discussion. When the mean free path is small compared with pore or tube dimensions, collisions between gas molecules are much more frequent than collisions of gas molecules with pore or tube walls, and the resistance is due to momentum transfer between gas molecules, or viscous "forces." The flow mechanism is "viscous flow" (5), and the driving force is the difference in total pressure. The distinction between partial pressure and total pressure is obviously not important when the gas phase is essentially pure water. As data to be presented later will show, the mole fractions of water in the vial and in the chamber are close to unity. The mole fraction of water vapor in the condenser, however, is significantly less than unity. Thus, if flow from the chamber to the condenser were predominantly Knudsen flow, the chamber resistance, defined using the total pressure difference between chamber and condenser as the driving force, might behave anomalously with variations in chamber pressure. However, as will be demonstrated later, the pressure dependence of the chamber resistance is of the expected form, and, therefore, the selection of the driving force seems appropriate.

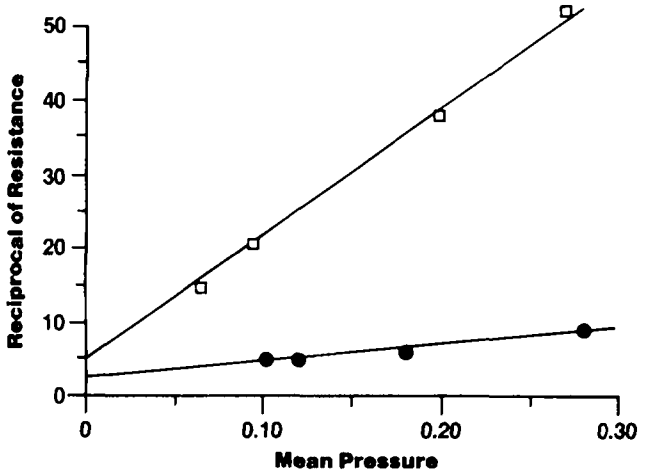

Figure 2—*Reciprocal of closure resistance* versus *pressure. Key: (□) 20-mm closure, (●) 13-mm closure.*

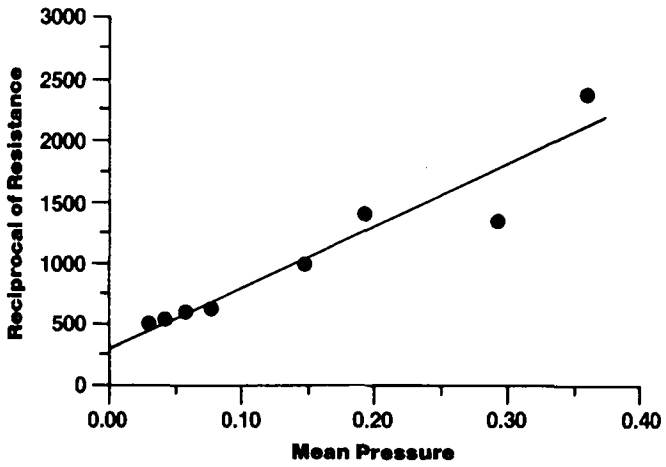

Figure 3—*Reciprocal of chamber resistance* versus *pressure.*

where K_c is the contribution resulting from direct conduction from shelf to glass at the points of contact, K_r is the contribution from radiative heat transfer, and K_g is the contribution from conduction through the gas between the shelf and the vial bottom. Both K_c and K_r are independent of pressure, but K_g increases with increasing gas pressure. Using the Smoluchowski theory as outlined by Dushman (5), and assuming the gap between the vial bottom and the shelf may be characterized by a constant "effective" distance, l, the gas conduction term may be written:

$$K_g = \frac{\alpha\Lambda_0 P}{1 + l(\alpha\Lambda_0/\lambda_0)P} \qquad \text{(Eq. 10)}$$

where Λ_0 is the free molecular heat conductivity of the gas at 0°C, λ_0 is the heat conductivity of the gas at ambient pressure, P is the gas pressure, and α is a function of the energy accommodation coefficient (a_c) and the absolute temperature of the gas (T):

$$\alpha = \frac{a_c}{2 - a_c} \cdot \sqrt{\frac{273.2}{T}} \qquad \text{(Eq. 11)}$$

The radiation term is a sum of two contributions, radiative heat transfer between the shelf and the vial bottom and radiative heat transfer between the shelf above the vial and the top of the vial. Radiative heat flow Q_r, depends on the difference in the fourth powers of the absolute temperatures of the two surfaces:

$$\dot{Q}_r = A_v \bar{e} \sigma (T_2^4 - T_1^4) \qquad \text{(Eq. 12)}$$

where σ is the Stefan-Boltzmann constant and $\bar{e}$ is the "effective" emissivity for the heat exchange, which depends on the relative areas of the two surfaces, their emissivities, and a geometrical view factor (4). For modest temperature differences between the two surfaces:

$$\dot{Q}_r \cong A_v \bar{e} \sigma 4\overline{T}^3 (T_2 - T_1) \qquad \text{(Eq. 13)}$$

where $\overline{T}$ is the mean temperature. For temperatures normally used in freeze-drying, the product, $\sigma 4\overline{T}^3$, is $\sim 1.0 \times 10^{-4}$. For radiation from the shelf upon which the vials rest (bottom radiation), the view factor is approximately unity, and since the emissivity of glass is near unity (4), the effective emissivity for bottom radiation is essentially the emissivity of the shelf surface, e_s, and T_1 is essentially the temperature at the vial bottom, T_b. For radiation from the top, the shelf area view factor of the vial top is much greater than the vial area, and one therefore expects (4) the effective emissivity to be essentially independent of the emissivity of the shelf above the vials. An exact evaluation of $\bar{e}$ for top radiation is not possible, and we treat the effective emissivity for top radiation, denoted e_v, as an experimental quantity to be evaluated by vial heat transfer experiments.

Since Q_r for top radiation is the heat transferred to the subliming ice, an empirically defined e_v should be based on an identification of T_1 as the temperature of subliming ice. In general, temperature differences within the product are small and, as a satisfactory approximation in most cases, T_1 may be taken as T_b. With the definitions of e_s and e_v given above, use of Eq. 13 and the approximation, $\sigma 4\overline{T}^3 \approx 1.0 \times 10^{-4}$, the radiative heat transfer coefficient, K_r, becomes:

$$K_r = 1.0 \times 10^{-4}(e_v + e_s) \qquad \text{(Eq. 14)}$$

In the case of vials resting on a tray bottom, an equation similar to Eq. 8 may be used to define a tray heat transfer coefficient, K_{TR}. Here the area, A_v, is replaced by the ratio of the tray area to the number of vials in the tray, and T_b is replaced by the temperature of the tray bottom. The meaning of $\dot{Q}$ and T_s is the same as in Eq. 8. The components of K_{TR} are given by the right side of Eq. 9, with the form of K_g identical to Eq. 10, although the value of the accommodation coefficient could differ from the value applicable to heat transfer between shelf and vial.

Since most of the heat input flows from the bottom of the vial to the subliming ice, the temperature of the product decreases as the distance from the bottom of the vial, X, increases. The usual proportionality between heat flow and temperature gradient may be used to define the effective thermal conductivity of the product, K_I:

$$\dot{Q}_B = -A_v K_I \cdot \frac{dT}{dX} \qquad \text{(Eq. 15)}$$

where $\dot{Q}_B$ is the heat flow (cal/s) through the bottom of the vial and T is the temperature of the frozen product in the vial. Since the total area available for heat transfer, A_v, is in part glass and in part frozen solution, one would expect K_I to be an area-weighted sum of the thermal conductivities of glass, κ_G, and frozen product, κ_p:

$$K_I \cong \frac{A_v - A_p}{A_v} \cdot \kappa_G + \frac{A_p}{A_v} \cdot \kappa_p \qquad \text{(Eq. 16)}$$

where A_p is the cross-sectional area of the frozen product calculated from the inner diameter of the vial. For dilute solutions, one would expect κ_p to be close to the value for pure ice (6, 7).

EXPERIMENTAL SECTION

Materials—Chemicals used were either reagent or USP grade and were used without further purification, except for filtration of the solutions prepared through a 0.45-μm filter to remove particulate matter. Solutions were prepared by weighing the appropriate quantities of distilled water and solute. Studies involving pure water used distilled water[2].

The rubber closures[3] have two openings for vapor passage in the semi-stoppered position. The 20-mm finish closure has two openings of ~0.4 cm in diameter, while the 13-mm finish closure has openings of ~0.2 cm in diameter.

The vials used were of commercial origin[4] and, except for the limited studies with 5304 vials, were selected to yield a representative cross section of vials produced during a given production run. All of the vials were type I glass; the 5303 and 5304 vials were molded and the others were tubing vials. The relevant vial geometric parameters are summarized in Table I. The contact-print parameters refer to the imprint created by first placing the vial bottom on an ink pad and then placing the vial on a sheet of paper resting on cardboard. Moderate pressure is applied by placing a 500-g weight on top of the vial. While reproducible, the thickness of the contact print is obviously procedure sensitive and does not represent, except in a relative sense, the actual area of physical contact between the vial and a hard surface. The entry in the last column, l_{max}, is the maximum separation distance between the vial bottom

[2] Water for Injection, Eli Lilly and Co.
[3] West Co.
[4] The vials with designation K were obtained from the Kimble Glass Co. and those with designation W were obtained from the Wheaton Glass Co.

Table II—Comparison of Resistances [a]

Product	Closure	Sublimation Rate, g/h[b]	Total Resistance, h·mm Hg/g	Relative Resistance, Percent of Total		
				Product	Closure	Chamber
KCl	None	0.523	1.38	91.5	0	6.5
KCl	20 mm	0.506	1.42	90.8	3.0	6.2
KCl	13 mm	0.458	1.56	82.7	11.7	5.6
I[c]	None	0.321	2.18	96.3	0	3.7
I	20 mm	0.315	2.22	94.6	2.0	3.4
I	13 mm	0.294	2.37	88.6	8.1	3.3

[a] Calculated for a vial of 3.8 cm^2 internal area, a dried product thickness of 0.5 cm, a chamber pressure of 0.1 mm Hg, an ice temperature of −20°C, and the laboratory freeze-dryer with a load of 60 vials of 4.7 cm^2 external area. [b] Sublimation rate per vial. [c] System I is dobutamine hydrochloride (dobutrex) and mannitol in a 1.12:1 weight ratio with total solids being 53 mg/mL.

and a flat surface, obtained simply by direct measurement with a metric ruler. Thus, this parameter is subject to a measurement error of ± ~0.02 cm.

Freeze-Dryers—The laboratory freeze-dryer was a highly modified commercial unit[5] (3) illustrated schematically in Fig. 1. A stainless steel cylinder (A) constituted the drying chamber wall, and the top of the unit (B) was a transparent plastic lid which formed a vacuum-tight seal with the chamber walls *via* a rubber gasket. Temperature control of the shelf (C) was provided by rapid circulation of fluid (methanol) from a thermostat (not shown) into the shelf (D) and out of the shelf (E); the fluid flowed through channels in the shelf interior. The chamber walls and top were covered with 2 cm of rubber foam insulation. However, under the usual conditions of ice sublimation, the dryer walls and top run warmer than the shelf. With a 5°C shelf, the walls were ~15°C while the top was ~12°C. The shelf surface used in these experiments was a thin (1-mm) metal plate in good thermal contact with the original shelf *via* a thin coat of high-vacuum silicone grease impregnated with copper dust. Unless specifically indicated otherwise, the shelf surface was a polished 316 stainless steel plate with a measured emissivity, e_s, of 0.28[6].

The temperature of the shelf surface was measured by thermocouple sensors (30-gauge wire) designed for surface temperature measurements. A welded copper-constantan thermocouple junction was silver-soldered to a copper disk ~1 mm thick and 1.5 cm in diameter. A 2-mm thick disk of foam insulation was glued to the copper disk, and an empty 10-mL glass vial was then glued to the insulation, thus insulating the thermocouple junction from the vial. Good thermal contact between the copper disk and the shelf surface was obtained by applying a thin coat of high-vacuum silicone stopcock grease to the bottom of the copper disk. The shelf surface temperature readings were accurate within ±0.5°C.

Without grease at the interface between the copper disk and shelf surface, the shelf sensors gave readings that were dependent on chamber pressure and were 2–3°C lower than the greased sensors. The shelf surface temperature was normally independent of position on the shelf, within ±0.5°C. The difference between fluid temperature and shelf surface temperature increased as the total sublimation rate increased (*i.e.*, increased heat flow), but was in the 1–2°C range for most of the experiments.

A butterfly valve (F) separated the drying chamber from a tube (G) (2.3 cm diameter, 25 cm length) leading to the condenser chamber (H). A tube (I) connected the interior of a modified vial with a pressure sensor external to the drying chamber (M1 or M2) by suitable manipulation of valves (K1, K2, K3, K4, and K5). A pressure-tight seal between the vial and a glass tube (I1) was made with silicone rubber glue. The glass tube was connected to a flexible stainless steel tube (I3) with a high-vacuum union[7]. The flexible tube was then connected with tube I *via* another high-vacuum union. Temperature measurements were made at four locations within the frozen product using copper-constantan thermocouples (30-gauge wire) (I4). Ten additional thermocouple leads (J) were also available. Differential capacitance manometers (M1, M2)[8] were used for quantitative measurements of absolute pressure, although a thermocouple vacuum gauge (N) was also included in the apparatus. Pressures and temperatures in the vial and chamber were continuously displayed as a function of time on a 24-channel recorder[9].

Studies requiring a larger shelf area than that available in the laboratory dryer were carried out using a pilot scale dryer[10] with condensers in the drying chamber. The dryer contained three shelves of 2800 cm^2 area separated from the condensers by radiation shields. Only the middle shelf was used in the experiments. The shelf surface was painted black and the surface temperature was uniform within 3°C: several shelf temperature sensors were used and care was taken to locate the sensors at positions where the average recorded temperature represented the true average shelf temperature. The temperature of the surface above the vials was colder than the shelf surface upon which the vials rested. Temperature measurements taken near the center of the top shelf indicated a mean difference of 4.3°C for the experiments performed.

Procedures—*Calibrations*—The differential capacitance manometers were calibrated against a precision McCloud gauge[11]. Deviations were less than the stated accuracy of the McCloud gauge (±3%) and no corrections were used. The thermocouple temperature sensors were calibrated at the ice point and at −25°C against a mercury-in-glass thermometer (±0.1°C).

Vapor Composition Measurement—Vapor composition was measured by comparing the pressure of a fixed quantity of vapor at room temperature with the corresponding pressure at dry ice temperature (−78°C), where the pressure of water is negligible. For example, the vapor composition in the vial was measured by first determining the total pressure in the vial with pressure gauge M1 (Fig. 1). Valves K1 and K2 were opened, valve K3 was closed, and the cold finger (O) was at ambient temperature. Next, valve K1 was closed to isolate the sample of vapor, representing the composition of vapor in the vial, and a dry ice–acetone bath was placed around the cold finger. Within a few minutes essentially all water vapor was condensed, and the residual pressure was due only to air[12]. This residual pressure was slightly lower than the air pressure in the original vapor since the air in the cold finger was at a lower temperature. The original air pressure was obtained from the measured residual pressure, using an empirically determined correction factor (1.044). The correction factor was determined by measuring the pressure reduction after placing the dry-ice bath on the cold finger at high pressure in a "dry" system, where essentially all the vapor was air. With the total pressure and the air pressure determined, the water vapor pressure in the sample was obtained by difference. The mole fraction of water in the vapor sample was calculated as the ratio of water partial pressure to the total pressure. When the pressure measurements were complete, the dry-ice bath was removed, and, by appropriate manipulation of valves, the vapor sample was pumped directly into the condenser chamber. The valves were then returned to their normal operating position for pressure monitoring. This procedure was believed to result in more rapid equilibration of the system following a composition measurement.

Mass Transfer Coefficients—Closure resistance at given mean pressure was determined by measuring the average pressure difference across the closure during sublimation of a known quantity of ice at constant chamber pressure. The mean pressure, $\bar{P}$, is the mean of the vial pressure and chamber pressure over the time interval of the experiment. The mean sublimation rate was calculated from the mass of ice sublimed and the time required for sublimation. The closure resistance was then obtained from Eq. 3. Similarly, the chamber resistance was evaluated from the chamber pressure, P_c, pressure in the condenser chamber, P_{cd}, and the total sublimation rate (all vials), $N \cdot \dot{m}$, using Eq. 4. Since both chamber and closure resistance measurements are sensitive to small pressure measurement errors (the pressure differences were small), care was taken to ensure that the pressure sensors (M1 and M2, Fig. 1) gave the same reading when connected to the same source, and a number of replicate experiments were made at each mean pressure to obtain the final data sets.

Heat Transfer Experiments—Two types of vial heat transfer experiments were performed. Experiments where data were collected on a single vial over a wide range of shelf temperatures and chamber pressures in a single experiment were denoted "single vial experiments." Experiments designed to measure both the mean heat transfer coefficient for a set of nominally identical vials and their corresponding standard deviation in heat transfer coefficients were referred to as "multivial experiments." All experiments, except those multivial experiments that used larger vials, were carried out using a full shelf

[5] Virtis Unitrap.
[6] Determined by adjusting the emissivity control on a hand-held optical pyrometer until the temperature readout of the instrument agreed with the thermocouple-measured surface temperature of the shelf.
[7] Cajon Ultra Torr Union; Cajon Co., Solon, Ohio.
[8] MKS Model 220 Baratron; MKS Instruments, Inc., Burlington, Mass.
[9] Esterline Angus Speed Servo II.
[10] REPP; Virtis Co.
[11] Kontes Glass Co., Vineland, N.J.
[12] The vapor pressure of ice at −78°C is only 0.6 μm.

Table III—Vapor Composition in Freeze-Drying [a]

Rate Per Vial, g/h	Shelf Temp., °C	Chamber Pressure, mm Hg	Mole Fraction of H_2O [b] Vial	Chamber
		Pure H_2O [c]		
0.23	−16	0.068	0.94	0.78 ± 0.08
0.26	−16	0.490 [d]	0.96	0.89
0.52	+12	0.093	0.96	0.78 ± 0.04
0.90	+12	0.493 [d]	0.97	0.94
		Mannitol, 50 mg/mL		
0.16	−21	0.045	0.85	0.78
0.22	−21	0.127 [d]	0.92	0.90
0.33	−21	0.228 [d]	0.95	0.92
0.42	− 6	0.232 [d]	0.95	0.93

[a] Full load of 60 vials (2.4 cm o.d.) in the laboratory freeze-dryer. [b] Estimated uncertainty ± 0.02 unless specifically indicated otherwise. [c] Mean of four replicate experiments. [d] Controlled air leak into the drying chamber.

of vials in the laboratory dryer. In both types of experiments, a small precision bore stainless steel tube (length 1.497 cm, 0.217 cm i.d.) was inserted in each stopper, and the stopper was inserted fully into the vial neck[13]. This procedure accomplished several purposes:

1. The pressure difference across the closure, which was needed to evaluate the sublimation rate in a single vial experiment, was increased over that found with stoppers in the usual semistoppered position, thereby decreasing the relative error in the pressure difference measurement.

2. The closure resistance was fixed by the geometry of the tube and the chamber pressure and, therefore, was not subject to variation arising from slight variations in stopper placement or geometry. Uniformity in resistance to mass transfer in a set of vials is critical when the standard deviation in heat transfer coefficient is measured.

The resistance of the metal tube used with the modified vial (Fig. 1) was determined as a function of mean pressure by a procedure identical to that used to determine closure resistance. The tube resistance, R_{TB}, is given by:

$$R_{TB}^{-1} = 0.2478 + 1.944\,\bar{P} \qquad \text{(Eq. 17)}$$

where $\bar{P}$ is $(P_v + P_c)/2$, and the numerical coefficients are a result of regression analysis of four data points over a range of $\bar{P}$ from 0.2 to 0.5 mm Hg, yielding a correlation coefficient of 0.9965. The numerical coefficients were in satisfactory agreement with the corresponding coefficients calculated strictly from theory[14].

A fill volume equivalent to a liquid depth of ~2 cm was used for all heat transfer studies. With pure water, a redistribution of ice within the vial occurred such that ice near the vial wall and ice near the thermocouple wire was preferentially removed. As a result of this phenomenon, measurements of temperature distribution in the ice had to be completed early in the experiment, before the assumption of a planar ice-vapor interface was seriously violated. Accurate temperature distribution data was obtained until ~15% of the ice had been removed. The vial heat transfer coefficient is defined assuming the ice at the vial bottom is in good thermal contact with the glass. Normally, with vials filled with pure water, partial loss of thermal contact occurs after sublimation of 35–50% of the ice. Thus, duration of a heat transfer experiment is limited to a time corresponding to sublimation of ~25% of the ice. Loss of thermal contact is rarely a problem when a frozen solution is dried.

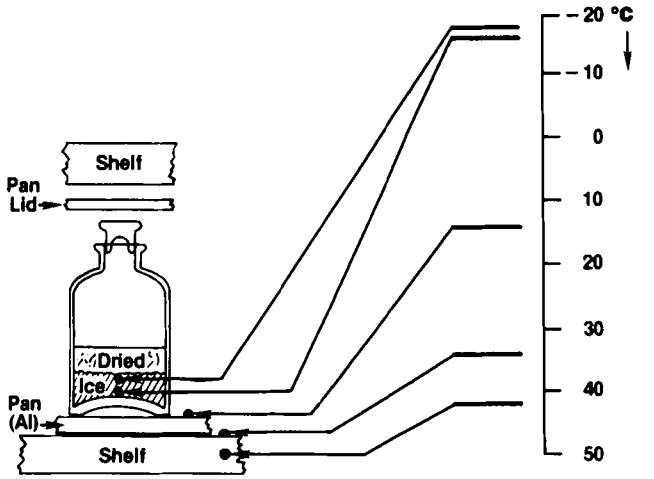

Figure 4—*Temperature profile in primary drying using dobutamine hydrochloride–mannitol (1:1) (10 mL) in 5304 molded vials (8.3 cm²) in an aluminum tray; heat flux = 42 cal/cm²·h, chamber pressure 0.10 mm Hg.*

[13] Experiments with the 5304 vials represented our first attempt at heat transfer coefficient measurement and used 13-mm freeze-drying stoppers in the semistoppered position.

[14] Using the theoretical relationships for gas flow in tubes (5), the resistance of the tube, in mm Hg·h/g, is given in terms of the tube cross-sectional area, A, tube radius, a, and tube length, l, by $R_{TB}^{-1} = [150 \cdot A\,(a/l)]/[1 + 8/3\,(a/l)] + 7965A\,(a^2/l)\bar{P}$. Substitution of the measured values of a and l (in cm) gives $R_{TB}^{-1} = 0.338 + 2.329\,\bar{P}$. While the agreement between theory and experiment is not quantitative, uncertainty in the measured value of a and uncertainty in the experimental coefficients could account for the difference.

Table IV—Evaluation of Heat Transfer by Top Radiation: Effective Emissivity, e_v

Product	N	A_v	$e_v \pm \sigma_m$
H_2O	7	4.71	0.83 ± 0.04
H_2O	3	6.83	0.94 ± 0.02
H_2O	3	17.2	0.79 ± 0.03
KCl (l = 0)	2	4.71	0.88
KCl (l = 0.3)	1	4.71	0.97
KCl (l = 0)	1	20.8	0.58
KCl (l = 0.2)	1	20.8	0.80
Mean			0.84

For single vial heat transfer studies, a representative vial from a given lot of vials was modified as shown in Fig. 1. After filling, normally with pure water, the modified vial and other vials of the same lot, all equipped with "identical" metal tubes, were loaded into the laboratory dryer, the liquid was frozen, and the chamber was evacuated. The procedure then involved a series of heat transfer measurements under steady-state conditions at selected shelf temperatures and chamber pressures. An operational definition of steady state is taken as constant temperatures (±0.2°C) and pressures (±2 μm) for a period of 10–15 min. The sublimation rate, $\dot{m}$, is calculated from the observed steady-state pressure readings using Eq. 3 with the closure resistance given by the tube resistance, Eq. 17. The heat transfer rate, $\dot{Q}$, is then calculated:

$$\dot{Q}\ (\text{cal/s}) = 0.1833\dot{m}\ (\text{g/h}) \qquad \text{(Eq. 18)}$$

where 660 cal/g is used for the heat of sublimation (8).

The first shelf temperature setting was adjusted to be equal to the ice temperature at the vial bottom. Heat transfer from the shelf to the vial was zero, and any residual heat transfer was due to radiative heat transfer from the dryer lid and/or possible contributions from conduction through the thermocouple wires and the pressure measurement tube (I, Fig. 1). Normally, shelf temperature settings of −10°C, 5°C, and 25°C were used in the balance of the experiment with four chamber pressures studied at each shelf temperature. The first pressure setting was the minimum pressure attainable with the leak valve closed (0.05–0.10 mm Hg). Higher pressures (0.2, 0.4, and 0.6 mm Hg) were obtained by manual adjustment of the controlled-leak valve (P, Fig. 1).

The advantages of the single vial experiment were that, during one ~6-h experiment, heat transfer could be studied over a wide range of shelf temperatures and chamber pressures, and the effect of radiation from the dryer lid could be directly measured. Since this procedure characterized the heat transfer for only one vial in a given experiment, the procedure was not designed to examine the variation in the heat transfer coefficient in a set of nominally equivalent vials. Moreover, it is difficult to select a "typical" vial and, even if this selection is successful, the presence of the pressure measurement tube makes it difficult to place the vial absolutely flat on the shelf with no downward force on the vial. Even a slight tilt of the vial would have decreased the area of actual contact between the glass and the shelf and would, therefore, decrease the contact conduction term, K_c (Eq. 9). The value of the separation distance, l (Eq. 10), may also be increased. Conversely, good contact with an excessive downward force on the vial may actually increase the value of K_c over that characteristic of a free-standing vial (9). Thus, particularly for the smaller vials where the contact problems were most severe, the single vial procedure was not the method of choice for determining the heat-transfer coefficient of an average vial in normal contact with the shelf.

Single vial data are, however, an accurate representation of the heat transfer for the vial used and the degree of vial–shelf contact experienced in the experiment performed. Thus, single vial data were used to efficiently and accurately investigate various assumptions in the defining equation for vial heat transfer coefficients (Eq. 8), to verify the theoretical form of the pressure dependence of K_v (Eqs. 9, 10), to characterize radiative heat transfer from the dryer lid, and to determine the effective thermal conductivity of the product (Eq. 15).

The equation defining the vial heat transfer coefficient, Eq. 8, assumes the

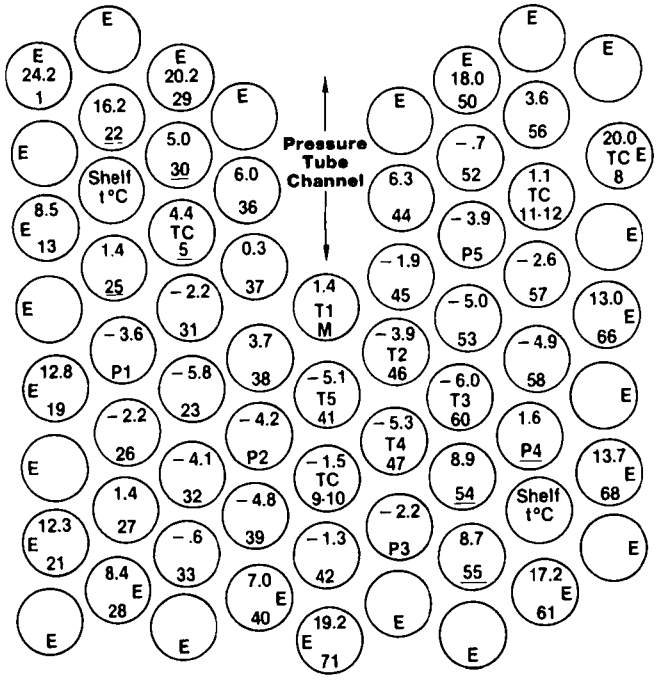

Figure 5—*Vial placement on the shelf and mean percent deviations in sublimation rates for components of the variance study. (See* Appendix I *for discussion.)*

temperature of the surface above the vials is the same as the temperature of the surface upon which the vials rest. While this assumption is valid for most freeze-dryers, the surface above the vials in the laboratory dryer (Fig. 1) was the chamber lid, which was not temperature controlled. Thus, the calculation of K_v from heat transfer data accumulated on the laboratory dryer involves a correction for the atypical radiative heat transfer from the dryer lid to the top of the vials. The heat transfer rate, $\dot{Q}$, for vials in the laboratory dryer may be written:

$$\dot{Q} = A_v(K_c + 1.10^{-4}e_s + K_g)(T_s - T_b) + A_v e_v \sigma(T_L^4 - T^4) \quad \text{(Eq. 19)}$$

where T_L is the lid temperature and T is the temperature of the subliming ice. The effective emissivity for top radiation (e_v) is assumed to be a property of the vial only. Thus, to convert heat transfer data from the laboratory dryer to K_v data defined by Eqs. 8 and 14, e_v must be evaluated.

Data for e_v were generated by using the single vial procedure and adjusting the shelf temperature so that $T_s = T_b$. Under these conditions, the heat transfer was due to the top radiation term only, and e_v data may be evaluated by determining $\dot{Q}$, T_L, and T. The value of T_L is obtained by direct measurement, $\dot{Q}$ is determined from P_v and P_c as outlined earlier, and T is calculated using one of the following procedures. When pure ice is in the vial, the resistance to mass transfer between the sublimation interface and the chamber is almost entirely due to the metal tube in the closure. The pressure in the vial, P_v, is essentially equal to the equilibrium vapor pressure of the subliming ice, and the temperature of the subliming ice, T, may be evaluated from the measured P_v data[15]. However, when a solution is freeze-dried, the vial pressure is much less than the equilibrium vapor pressure of ice, and the value of T is calculated using the measured product temperature near the sublimation interface[16].

Multivial heat transfer studies were used to determine the mean vial heat transfer coefficient as a function of pressure as well as to obtain the standard deviation in heat transfer coefficients for a set of nominally equivalent vials. All vials investigated were filled with pure water to a depth of ~2 cm, and each vial was weighed (±0.2 mg). After loading and freezing, the shelf temperature

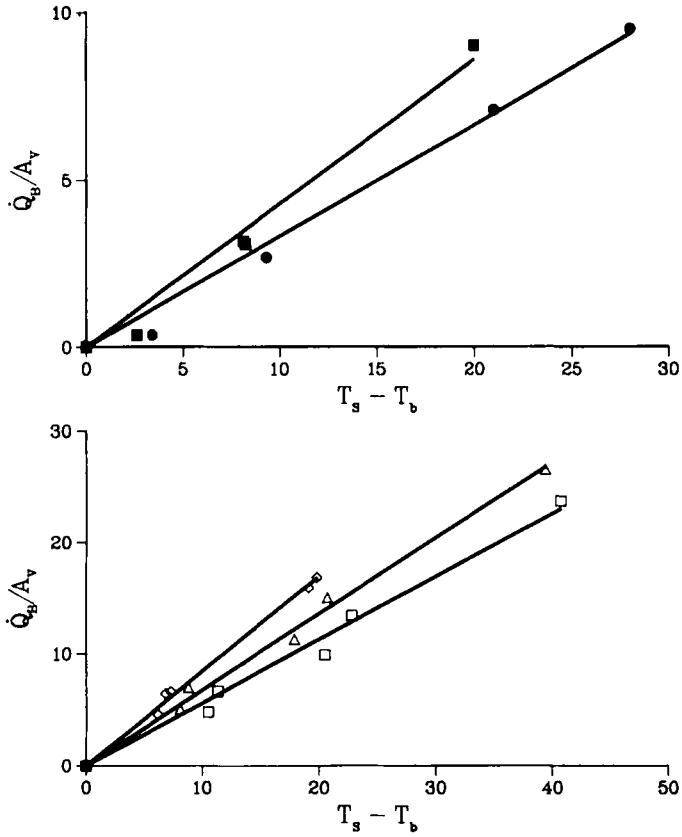

Figure 6—*Proportionality between heat transfer rate and temperature difference. Key: 5303 vials, (●) 0.1 mm Hg and (■) 0.2 mm Hg; W5800 vials, (□) 0.2 mm Hg, (△) 0.4 mm Hg, and (◇) 0.6 mm Hg.*

(and product temperature) were adjusted to the expected steady-state sublimation temperature for that experiment, and the chamber was quickly evacuated to the desired chamber pressure by manual adjustment of the leak valve. Once the pressure decreased below ~1 mm Hg and sublimation began, the shelf temperature was quickly increased to +5°C. The entire experiment was conducted under conditions of constant shelf temperature (5°C) and constant chamber pressure. After ~2 g of ice was sublimed, the dryer was vented, and each vial was weighed to obtain the mass loss for each vial. The average sublimation rate for each vial is calculated as the mass loss divided by the time period of sublimation. Calculations of the heat transfer coefficients and the corresponding standard deviation from the raw sublimation rate and temperature data are described in *Appendix I.*

RESULTS AND DISCUSSION

Closure Resistance—Two types of closures of similar design were studied. The smaller closure was designed for use with vials that had 13-mm o.d. necks, while the larger closure was used with vials that had 20-mm o.d. necks. Both closures had two openings in the semistoppered position with effective diameters of 0.2 cm for the 13-mm size and 0.4 cm for the 20-mm size. The experimental data (Fig. 2) demonstrate that the reciprocal of closure resistance is a linear function of mean pressure, as expected (Eq. 7). The mean pressure is the mean of the vial and chamber pressures. Each point is the mean of at least two replicate experiments, while the solid lines represent smoothed data from Eq. 7 with the coefficients determined by regression analysis:

$$R_s^{-1} = 2.3 + 22.4\bar{P} \text{ (13 mm)} \quad \text{(Eq. 20)}$$

$$R_s^{-1} = 4.8 + 169\bar{P} \text{ (20 mm)} \quad \text{(Eq. 21)}$$

The resistance of the 13-mm closure was roughly a factor of 5 higher than the 20-mm closure at corresponding pressures over the pressure range normally encountered in practice, a ratio close to that predicted theoretically[17]. The

[15] The vapor pressure of ice, in mm Hg, as a function of absolute temperature (8), may be expressed as $\ln P = -6144.96/T + 24.01849$.

[16] Although we cannot directly measure temperature at the sublimation interface, the temperature variation within the product is negligible between locations where temperature is measured (Fig. 1); thus, both methods of determining T should yield the same result when the product is pure water. However, we find that the value of T determined from P_v is systematically ~1.8°C lower than the corresponding measured product temperature. Evidently, a temperature gradient exists very near the sublimation surface, at least when the sample is pure water. However, a temperature error of 1.8°C produces an error in e_v of only 0.03, so even if the same error is present with a solution, the error introduced into the e_v data is slight.

[17] If each closure opening is approximated as a tube of radius a and length l, the same equation used to calculate resistance of the metal tubes[14] may be used to estimate the coefficients in Eq. 7. The estimated values of a and l are $a = 0.2$ cm, $l = 0.4$ cm (20 mm) and $a = 0.1$ cm, $l = 0.3$ cm (13 mm). Thus, the theoretical equivalents of Eqs. 20 and 21 are $R_s^{-1} = 1.7 + 17\bar{P}$ (13 mm) and $R_s^{-1} = 8.1 + 200\bar{P}$ (20 mm).

Table V—Vial Heat Transfer Coefficients for 10-mL Vials (A_v = 4.71 cm²) in Laboratory Dryer

Experiment	Vial	Chamber Pressure, mm Hg	Mean $\dot{m}$, g/h	$\hat{\sigma}(\dot{m})$, %	$10^4 K_v$, cal/s·cm²·°C	$\sigma(K_v)$, %
			Polished Stainless Steel Shelf Surface			
R[a]	W5800	0.2	0.3782	4.5	6.19	5.1
1[b]	W5800	0.1	0.3472	3.7	4.89	2.0
1[b]	K5800	0.1	0.3727	4.8	5.45	5.2
2[b]	W5800	0.2	0.4061	3.3	6.10	2.1
2[b]	K5800	0.2	0.4339	4.2	6.78	4.7
3[b]	W5800	0.4	0.4509	3.9	7.89	4.6
3[b]	K5800	0.4	0.4824	4.5	8.83	6.1
4[b]	W5800	0.1	0.3440	4.0	4.79	2.8
4[b]	W5811	0.1	0.3632	3.9	5.21	2.9
5[b]	W5800	0.2	0.4051	3.9	6.17	3.8
5[b]	W5811	0.2	0.4335	4.1	6.86	4.4
6[b]	W5800	0.4	0.4508	3.2	7.69	2.8
6[b]	W5811	0.4	0.4849	3.0	8.65	2.4
			Painted Black Shelf Surface			
7[c]	W5811	0.2	0.4451	4.7	7.43	6.1

[a] Mean data from six replicate experiments; N = 36, A = 5; SD in calculated $10^4 \times K_v$ is ±0.14; N is the total number of vials in the sample and A is the number of vials located adjacent to a shelf temperature sensor (see *Appendix I* and Fig. 5). [b] N = 15, A = 6. [c] N = 35, A = 12.

intercept (Fig. 2) at $P = 0$ represents the contribution of Knudsen flow, and the ratio R_s^{-1} ($P = 0$) to R_s^{-1} at any given pressure represents the relative contribution of Knudsen flow to the total vapor flow at that pressure. Thus, at >0.03 mm Hg for the 20-mm closure and >0.1 mm Hg for the 13-mm closure, Knudsen flow was <50% of the total flow, and the flow mechanism became predominantly viscous flow or bulk-fluid flow.

Chamber Resistance—The reciprocal of the chamber resistance of the laboratory dryer is a linear function of the mean pressure (the mean of the chamber and condenser pressures) within the precision of the data (Fig. 3). Each data point is the mean of at least two, and usually more than four, replicate experiments. The solid line gives the best fit of the data to Eq. 7 with $a_0 = 320 \pm 230$ and $a_1 = 4960 \pm 650$, where the uncertainty represents the standard error in the coefficient. As with closure resistance, the intercept (Fig. 3) at $P = 0$ represents the contribution of Knudsen flow while the ratio R_c^{-1} ($P = 0$)/R_c^{-1} gives the relative contribution of Knudsen flow to total vapor flow. Due to the considerable uncertainty in the experimental value of a_0, it is not possible to make a definitive comment on the relative contribution of Knudsen flow.

Assuming that the chamber resistance is due entirely to the tube separating the chamber from the condenser, theoretical values of a_0 and a_1 may be calculated[14]: a_0 = 124 and a_1 = 28,639. While the experimental and theoretical values of a_0 agree within the uncertainty in the data, the experimental value of a_1 is a factor of ~6 less than the theoretical estimate. Thus, the pressure-dependent term in R_c^{-1}, which is due to the viscous flow mechanism, was much smaller than expected, and the resistance to viscous flow in the laboratory dryer appeared to be anomalously high.

Since the chamber resistance depends on the dryer dimensions, the chamber resistance of a production scale dryer obviously will be much less than the chamber resistance of the laboratory dryer. However, the total resistance to flow from a given vial (Eq. 6) depends on the scaled chamber resistance, NR_c, where N is the number of vials in the dryer. The pressure drop between chamber and condenser for a given sublimation rate per vial depends on the scaled chamber resistance (Eq. 4). If the laboratory dryer is a satisfactory model for a production scale dryer, the scaled resistances should be comparable for the two dryers. Although sparse, the production data available suggest that at a mean pressure of 0.1 mm Hg, the scaled chamber resistance (N = 30,000) is ~0.05 mm Hg·h/g, while the corresponding scaled resistance for the laboratory dryer (N = 70) is 0.086 mm Hg·h/g.

Comparison of Resistances—Using the data presented in Figs. 2 and 3 and dried product resistances generated from vial data in a previous study (3), the resistance to passage of water vapor from the sublimation surface in a given vial to the condenser chamber may be calculated for each barrier: dried product, closure, and chamber–condenser pathway. The mean pressures needed to evaluate closure and chamber resistances are evaluated by solving Eqs. 1, 3, and 7 or Eqs. 1, 4, and 7, with 0.1 mm Hg as the chamber pressure.

The dried-product resistance was the dominant resistance, accounting for nearly 80% of the mass transfer resistance even when the small (13-mm) closures were used (Table II). Closure and chamber resistances were of the same order of magnitude, the chamber resistance was less than the resistance of a 13-mm closure, but greater than the resistance of a 20-mm closure.

Vapor Composition—The gas present in the vial and the chamber was mostly water vapor under all conditions studied (Table III). Even when the chamber pressure was increased by a controlled air leak, the vapor in the chamber was predominantly water. These observations, which are in qualitative agreement with literature data (10), are a direct result of the low pumping speed of the system for air relative to the pumping speed for a considerable vapor (H_2O). An air leak increases the total pressure in the condenser chamber (mostly air) and, because the chamber pressure is related to the condenser pressure by Eq. 4, the chamber pressure also increases. However, even with an air leak sufficient to increase the condenser pressure significantly, the molar flow rate of air is still much smaller than the molar flow rate of water vapor, and the chamber gas is, therefore, predominantly water. Thus, as a first approximation, the heat conductivity parameters Λ_0 and λ_0 (Eq. 10) refer to water vapor.

Temperature Profile in Primary Drying—A temperature profile measured during primary drying in the pilot dryer is illustrated by Fig. 4. In this experiment, the vials were placed in an aluminum tray with a flat 5-mm thick bottom and a tray lid containing open channels for vapor passage. Only the middle shelf was used. The temperature data (Fig. 4) refer to mean temperatures recorded at 50% completion of primary drying, and the heat transfer rate is the average heat transfer rate calculated from the total amount of ice sublimed and the primary-drying time.

Heat transfer may be described in terms of four barriers or resistances to heat flow: (*a*) the shelf itself, with a temperature difference of 8°C between the shelf interior and the shelf surface; (*b*) the pan or tray, with a temperature

Table VI—Vial Heat Transfer Coefficients for 20-mL Vials (A_v = 6.83 cm²) in Laboratory Dryer[a]

Experiment	Vial	Chamber Pressure, mm Hg	$\dot{m}$, g/h	$\hat{\sigma}(\dot{m})$, %	$10^4 K_v$, cal/s·cm²·°C	$\sigma(K_v)$, %
1	W5816	0.068	0.3664	3.4	3.47	4.0
1	K5816	0.068	0.3875	3.5	3.79	4.2
2	W5816	0.100	0.4209	3.2	4.22	3.8
2	K5816	0.100	0.4503	4.0	4.69	5.1
3	W5816	0.200	0.4879	3.0	5.40	3.6
3	K5816	0.200	0.5285	4.0	6.14	5.5
4	W5816	0.400	0.5520	2.3	6.89	2.4
4	K5816	0.400	0.6113	3.2	8.18	4.4
5	K5816	0.400	0.6159	4.7	8.13	6.9

[a] Polished stainless steel shelf. A = 0; N = 14 (K5816), N = 13 (W5816); see Table V footnote *a* for definitions of A and N.

Table VII—Vial Heat Transfer Coefficients for 100-mL 5303 Vials (A_v = 17.2) in Pilot Dryer [a]

Experiment	Chamber Pressure, mm Hg	$\dot{m}$, g/h	$\hat{\sigma}(\dot{m})$, %	$10^4 K_v$, cal/s·cm²·°C	$\sigma(K_v)$, %
1	0.100	0.5342	4.1	3.1	3.0
2	0.200	0.7470	4.0	4.2	3.3
3	0.200	0.7968	3.0	4.6	1.7
4	0.400	0.7696	4.2	5.0	3.8

[a] Both W5303 and K5303 vials gave the same mean K_v (within 0.2%), and $\hat{\sigma}(\dot{m})$ is essentially the same for the pooled data set as for each data set considered individually.

difference of 20°C between the shelf surface and the top surface of the tray bottom; (*c*) the vial, with a temperature difference of 30°C between the pan surface and the product in the bottom of the vial; and (*d*) the frozen product, with a temperature difference of ~2°C between the ice at the vial bottom and the ice at the sublimation interface. The thermal resistance of a barrier may be defined as the ratio of temperature difference across the barrier and the area-normalized heat flow (4). Thus, the largest thermal resistance (50%) is the vial-tray interface, but both the tray-shelf interface and the shelf itself contribute significantly to the total resistance, 33.3 and 13.3%, respectively.

As defined here, the thermal resistance of the vial includes the thermal resistance of the glass in the vial bottom. Likewise, the tray resistance includes the thermal resistance of the aluminum in the tray bottom. However, as shown by Nail (4), the thermal resistance of the metal in an aluminum tray bottom is essentially zero. Therefore, the tray resistance is due to the tray-shelf interface resistance. The thermal resistance of the glass, even for molded vials where the glass is several millimeters thick, is generally less than the thermal resistance of the frozen product (4), and the vial thermal resistance is nearly all due to the tray-vial interface resistance. In Fig. 4, the thermal resistance of the glass (3.5 mm thick) is ~5% of the defined vial resistance and <3% of the total thermal resistance. For tubing vials, the glass thickness is usually ~1 mm, and the corresponding contribution of the glass to thermal resistance is even less. Consequently, the thickness of the glass is not a significant factor in vial heat transfer and the usual variations in glass thickness may be ignored.

Heat transfer coefficients for the tray, K_{TR}, and the shelf itself, K_S, may be defined by equations analogous to the defining equation for vial heat transfer coefficients (Eq. 8). Theoretically, the tray heat transfer coefficient may be described as a sum of contact, radiation, and gas conduction terms (Eq. 9), where the gas conduction term depends on pressure in the same manner as the corresponding term in the vial heat transfer coefficient (Eq. 10). For the aluminum tray studied, the tray temperature is uniform throughout the tray bottom, and the calculated value of $K_{TR} = 5.8 \times 10^{-4}$ cal/s²·cm²·°C at 0.1 mm Hg. Similar measurements with a stainless steel tray of the same geometry, but with a warped bottom (with ~4 mm maximum distance between the shelf and the tray bottom) showed significant tray temperature differences (≈5°C) between zones over a maximum warp and zones near a shelf-tray contact point. The mean tray heat transfer coefficient at 0.1 mm Hg is 3.3×10^{-4} cal/s·cm²·°C, but in a zone of maximum warp, the coefficient decreased to 2.4×10^{-4} cal/s·cm²·°C.

The shelf heat transfer coefficient, K_S, calculated from the temperature difference between shelf interior and shelf surface (Fig. 4) is 1.5×10^{-3} cal/s·cm²·°C. The reciprocal of K_S is the thermal resistance for flow of heat from the shelf interior to the surface and probably represents a combination of limited fluid flow through the shelf interior and a finite thermal conductivity of the shelf material itself. Thus, the shelf heat transfer coefficient is expected to be independent of chamber pressure and is probably quite sensitive to dryer design.

Vial Heat Transfer: Radiation Effects/Driving Force for Heat Flow—*Contribution of Radiation*- The parameter, e_v, represents the effect of radiation heat transfer from the surface above the vials. The e_v data obtained (Table IV) show no systematic trend as the vial size (value of A_v) increased[18]. The experiments with potassium chloride were carried out to determine whether the development of a dried-product layer above the sublimation interface would act as a thermal barrier and reduce the heat transfer *via* top radiation. Thus, measurements of e_v were made at the beginning of sublimation where the dried-product thickness, l, is essentially zero, and later in the same experiment after a dried product layer developed ($l > 0$). The data clearly do not show a decrease in e_v as l increases; indeed, there appears to be a small increase in e_v as l increases, a result for which we cannot offer a reasonable interpretation. In summary, the data appear to be adequately interpreted in terms of a value of e_v equal to 0.84, independent of vial size and thickness of the dried-product layer.

The definition of the vial heat transfer coefficient assumes the vial is completely surrounded by other vials. Clearly, this assumption is not valid for those vials forming the perimeter of a group of vials. Such "edge" vials may show a significantly higher sublimation rate than "interior" vials due to radiative heat transfer from the surface facing the vial perimeter. The additional heat transfer rate for edge vials, $\Delta\dot{Q}_E$, may be written:

$$\Delta\dot{Q}_E = A_c e_E \sigma (T_w^4 - T_b^4) \qquad \text{(Eq. 22)}$$

where A_c is the vial area exposed to the extra radiation effects, taken as one-half the cylindrical area of the vial, T_w is the absolute temperature of the heat source (*i.e.*, the chamber wall), and T_b is the absolute temperature of the product. The parameter, e_E, denotes the effective emissivity for radiative heat transfer between the edge vial and the heat source. Numerical analysis[19] of the experimental data (Appendix I; Fig. 5) yields, $e_E = 0.21$. Since edge vials are atypical, edge vial data are excluded from heat transfer data analysis.

Proportionality Between Heat Transfer Rate and Temperature Difference—The definition of the vial heat transfer coefficient assumes that the heat transfer rate is proportional to the temperature difference between the shelf surface and the temperature in the product at the bottom of the vial (Eq. 8). Thus, the driving force for heat flow is taken as the temperature difference, $T_s - T_b$. The corresponding assumption for heat transfer in the laboratory dryer is a direct proportion between heat transfer rate from the shelf, denoted $\dot{Q}_B$, and the same temperature difference. The value of $\dot{Q}_B$ is obtained from the total heat transfer rate by subtraction of the top radiation contribution. The top radiation contribution is calculated using the term in Eq. 19 involving e_v with $e_v = 0.84$. Data are obtained at constant pressure as a function of $T_s - T_b$ by varying the shelf temperature in single vial studies. Representative results for two types of vials are shown in Fig. 6 at selected chamber pressures. As expected, $\dot{Q}_B$ is directly proportional to $T_s - T_b$ within the uncertainty in the data. Further, the slopes of the plots were observed to increase as the chamber pressure increased, which is consistent with the expected increase in conduction through the vapor phase as pressure increases.

Vial Heat Transfer Coefficients *Phenomenological Results*—The results of the multivial studies (Tables V-VII) are identified by experiment number (first column), vial type (second column), and chamber pressure (third column). In general, two vial types were studied in the same experiment, thereby providing greater accuracy for the comparison of K_v between the two vial samples under identical conditions. Thus, while the precision in K_v for a given set of vials is ± ~2%, as measured by the standard deviation in a series of replicate experiments (laboratory dryer), the ratio of K_v data for the two sets of vials is precise within ± ~0.5%.

The vial number (*e.g.*, 5800) defines the vial specifications while the letter (*i.e.*, W or K) defines the supplier. Thus, although W5800 and K5800 vials are nominally identical, vial heat transfer coefficients for K5800 vials are significantly higher than K_v for W5800 vials at corresponding pressures (Table V). For the 5800 vials studied, the K_v ratio is 1.115, independent of pressure within ±0.5%. The analogous K_v ratios for 5816 vials (Table VI) increases smoothly from 1.092 at 0.068 mm Hg to 1.187 at 0.4 mm Hg. Again, although both W5816 and K5816 vials are nominally identical, the K vials have significantly higher vial heat transfer coefficients than the W vials. Contrary to the K *versus* W bias found for tubing vials (5800 and 5816), the large molded 5303 vials studied show no supplier bias in K_v (footnote *a* in Table VII). The mean K_v values are identical, within ±0.2%, for K5303 and W5303 vials at corresponding pressures.

The mean K_v data reported are evaluated using a finite number of vials

[18] If a significant amount of heat were conducted down the thermocouple wires or through the pressure measurement tube, a term in Eq. 19, independent of vial area, would be needed. The experimental value of e_v would include a term inversely proportioned to A_v, which would then result in the measured e_v data decreasing as A_v increases. Regression analysis of all the pure water data (13 experiments) gives: $e_v = 0.82 + 0.14/A_v$, with a correlation coefficient of 0.10. Thus, heat conduction through the thermocouple wires (30-gauge) and/or the pressure measurement tube is small and may be ignored.

[19] Under the conditions of the experiment (*Appendix I*), the 15.0% sublimation rate bias between edge vials and interior vials yields $\Delta\dot{Q}_E = 0.0106$ cal/s. The W5800 vial is a cylinder of height ~4 cm and radius 1.22 cm. The observed value of T_b is 254.7 K. Since the shelf is actually a shallow box with a height of 1 cm, the heat source is the shelf, 275.5 K, for the first 1 cm of vial height and is the chamber wall, 288 K, for the remaining 3 cm of vial height. Thus, $\Delta\dot{Q}_E = \pi(1.22)e_E \cdot \sigma[1\cdot(275.5^4 - T_b^4) + 3\cdot(288^4 - T_b^4)]$, and the calculated value of e_E is 0.21.

Table VIII—Vial Heat Transfer Parameters[a] with Accommodation Coefficient, a_c, of 0.67 and Effective Top Emissivity, e, of 0.84

Vial	Contact Parameter 10^4K_c	Separation Distance (l), cm
W5800[b]	1.24 ± .08[e]	0.0471 ± 0.0018[e]
K5800[b]	1.70 ± 0.11	0.0396 ± 0.0021
W5811[b]	1.58 ± 0.11	0.0395 ± 0.0021
W5816[b]	0.63 ± 0.08	0.0513 ± 0.0024
K5816[b]	0.87 ± 0.08	0.0372 ± 0.0013
5303[c]	0.4 ± 0.4	0.090 ± 0.028
5304[d]	0.7 ± 0.2	0.067 ± 0.008

[a] Parameters evaluated using heat conductivity values for pure water taken from the literature (5, 11): $\Lambda_0 = 6.34 \cdot 10^{-3}$ cal/s·cm²·°C·mm Hg; $\lambda_0 = 4.29 \times 10^{-5}$ cal/s·°C·cm. [b] Data from multivial studies (Tables V and VI). [c] Datum is mean of the multivial study ($10^4K_c = 0 \pm 0.6$, $l = 0.103 \pm 0.040$) and the single vial study ($10^4K_c = 0.8 \pm 0.1$, $l = 0.078 \pm 0.009$). [d] Datum from the single vial studies with two vials. [e] Uncertainty given is the standard error of the parameter as given by the MLAB program output and does not reflect absolute error. The value of K_c is sensitive to the choice of a_c and also depends on the mathematical form chosen for K_g.

(normally ~15) randomly selected from one lot of vials. Thus, the reported K_v value is an accurate representation of the mean of the lot within a standard error, $\sigma(K_v)/\sqrt{N}$, where N is the number of vials studied. Using the $\sigma(K_v)$ data reported, the corresponding standard error in the K_v ratio between K vials and W vials averages ~1.5%. Therefore, the K_v ratios calculated from the reported data are an accurate representation of the lots studied, within ~1.5%, and probably reflect differences in geometry of the vial bottoms (Table I). Vial heat transfer data for different lots from the same supplier are needed to verify that the lots investigated in this study are typical of the total output from a given supplier. At present, such data are not available, but the differences in vial bottoms noted in Table I appear to be consistent, suggesting that the K_v ratios determined in this study do indeed indicate a supplier difference rather than a lot-to-lot variation within a given product.

The differences in K_v between K and W vials are of no practical significance in freeze-drying, as long as vials from only one supplier are used for a given product. A slightly lower K_v simply requires a slightly higher shelf temperature in the freeze-drying process. The supplier bias is particularly important if circumstances can arise where both K and W vials are used for the same pharmaceutical product lot. Since the K *versus* W bias in K_v is significantly greater than nonuniformity in K_v for a given vial type, measured by $\sigma(K_v)$, a significant increase in nonuniformity of heat input would result whenever both K and W vials are used in the same freeze-drying run. The consequence could well be a large product loss arising from collapse or eutectic melt, although the severity of the problem encountered would depend on both the nature of the product and the process design.

The relative standard deviation in K_v, $\sigma(K_v)$, is a measure of the uniformity of heat transfer coefficients within a given lot of vials. Since the $\sigma(K_v)$ data are based on data from a relatively small number of vials (~15), one expects a sizable uncertainty in a given value of $\sigma(K_v)$[20]. Based on the differences in $\sigma(K_v)$ between replicate experiments (Tables V–VII), the uncertainty (SD) in a reported value of $\sigma(K_v)$ is ~1.2%.

While the $\sigma(K_v)$ data are only semiquantitative, several generalizations appear valid. First, all vial types have a surprisingly uniform heat transfer coefficient; the average value of $\sigma(K_v)$ is only 4%. Second, the uniformity in K_v is systematically slightly better for W tubing vials than for the corresponding K vials (Tables V and VI). The data for 5800 and 5816 vials show a mean $\sigma(K_v)$ of 3.4 ± 0.3% for W vials, while the corresponding value for K vials is 5.3 ± 0.3%. The uncertainties given are standard deviations of the means. Third, while a small but significant pressure dependence in $\sigma(K_v)$ could be obscured by the scatter of the data, the data are not consistent with a pressure dependence of more than a factor of ~2 over the pressure range studied. The pressure dependence in $\sigma(K_v)$ will be addressed later from a theoretical point of view.

While histograms constructed from the sublimation rate data do appear consistent with a normal distribution of K_v data in a set of vials, the data available are not sufficient for a critical test. Experiments involving a very large number of vials in a freeze-dryer with no significant position effects would be needed for a definitive study of the distribution function. Thus, one should exercise caution in assuming a normal distribution for the vial heat transfer coefficients.

Mechanisms of Heat Transfer—In principle, the contribution of each of the parallel mechanisms of heat transfer from shelf to vial may be evaluated by regression analysis of K_v data as a function of pressure using the mathematical model defined by Eqs. 9–11 and 14. The zero pressure intercept of K_v *versus* pressure defines the sum of the radiative and the contact conduction contributions. The radiative contribution (Eq. 14) is evaluated independently by evaluation of the effective emissivity for top radiation, $e_v = 0.84$ (Table IV), and by measurement of the emissivity of the shelf surface (0.28 for polished stainless steel, 0.95 for painted black shelf). The contact contribution, K_c, is calculated from the zero pressure intercept of K_v and the calculated value of the radiative contribution, K_r. Both heat conductivity parameters, Λ_0 and λ_0, are available from the literature (5, 11). The gas conduction term, K_g (Eq. 10), is therefore determined by the accommodation coefficient, a_c (Eq. 11) and the effective mean separation distance between the bottom of the vial and the shelf, l. Thus, three parameters, K_c, a_c, and l, are determined by regression analysis of the data. However, the multivial K_v data set for any type of vial consists of K_v values at only three or four different pressures, which is insufficient data to evaluate the three parameters with acceptable accuracy. In theory (12), the accommodation coefficient is a function of the natures of the gas, the shelf surface, and the vial surface. The gas is independent of the vial studied, the vial surface is always glass, and, with the exception of one study with the pilot dryer, the shelf surface is polished stainless steel. Therefore, the accommodation coefficient is assumed to be a constant and is evaluated by simultaneous regression analysis of all data sets, where K_c and l are vial specific, but the accommodation coefficient is independent of the type of vial. Both single vial-generated data, fit to Eq. 19, and multivial data, fit to Eqs. 9–11 and 14, were used to determine the accommodation coefficient. Although single vial data may yield inaccurate values of K_c and l (see *Experimental Section*), these data are suitable for evaluation of the accommodation coefficient.

Table IX—Vial Heat Transfer: Comparison of Heat Transfer Mechanisms for Vials on a Polished Stainless Steel Shelf

Vial	Contribution to Heat Flow, % of Total					
	P = 0.1 mm Hg			P = 0.4 mm Hg		
	Radiation	Contact	Gas	Radiation	Contact	Gas
K5800	21	32	47	13	19	68
W5816	27	16	57	16	9	75
5303	32	11	57	22	8	70

Single vial heat transfer data for the 5303, W5816, W5800, K5800, and W5811 vials are well represented by the theoretical model (Eq. 19) with a single accommodation coefficient of 0.72 ± 0.07. The uncertainty given is the standard error provided by the MLAB[21] fit program. The data are the result of replicated experiments consisting of 132 data points at chamber pressures from 0.06 mm Hg to 0.6 mm Hg and at shelf temperatures from −15°C to 25°C. The computer fit provided 11 parameters, including the accommodation coefficient, with a relative SD in $\dot{Q}$ of 7.7%, which is within the anticipated

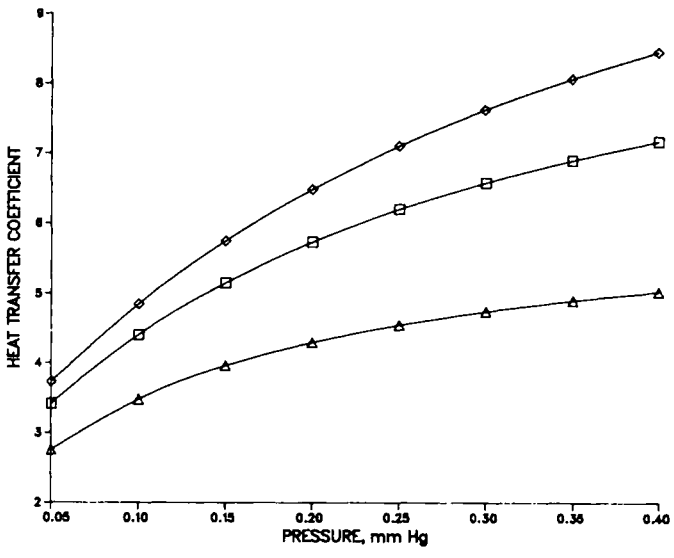

Figure 7—*Pressure dependence of vial heat transfer coefficients for selected vials. Key: (□) W5816, (◇) K5816, and (△) 5303.*

[20] The variance in a standard deviation estimate based on N measurements is approximately $\sigma^2/2N$ (14), where σ^2 is the variance in the measured quantity. Thus, the SD in $\hat{\sigma}(\dot{m})$ is $\approx \hat{\sigma}(\dot{m})/\sqrt{2N}$. Assuming that in the evaluation of $\sigma(K_v)$ from $\hat{\sigma}(\dot{m})$, the only uncertainty of consequence originates in the uncertainty in $\hat{\sigma}(\dot{m})$; numerical calculations give 1.6% for the average uncertainty (SD) in $\sigma(K_v)$.

[21] MLAB is a general purpose model fitting a computer program package available from the Division of Computer Research and Technology, National Institutes of Health, Bethesda, Md.

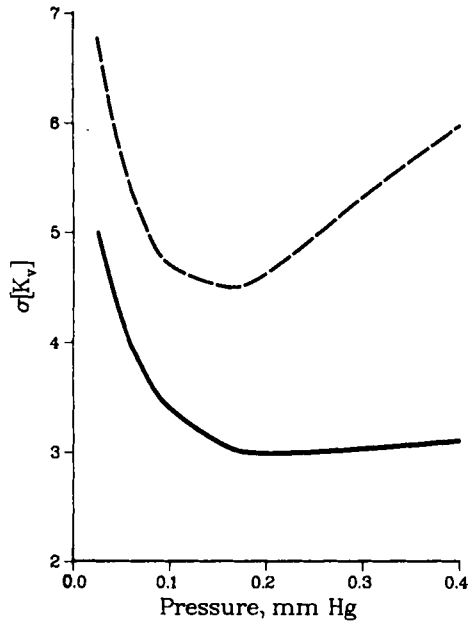

Figure 8—*Calculated pressure dependence of the relative standard deviation in vial heat transfer coefficients. Key: (—) mean of W tubing vials, and (- - -) mean of K tubing vials.*

experimental error. The multivial data set, consisting of 22 (K_v, P) data pairs, is also well represented by the theoretical model. Eleven parameters, including a single accommodation coefficient, $a_c = 0.62 \pm 0.05$, are obtained. The *SD* of the fit for 10^4K_v is ±0.10, which is within the precision of the data. The agreement between the single vial results and the multivial results for a_c is satisfactory, and the mean value, 0.67, is taken as the effective accommodation coefficient for vial heat transfer. When a_c is fixed at 0.67, and the regression analysis of single vial and multivial data are repeated, the quality of the fit obtained is essentially identical to that found when a_c is an adjustable parameter. The resulting K_c and l parameters are listed in Table VIII.

Since multivial data are generally a more accurate representation of the heat transfer characteristics of the mean of a set of vials, only multivial-derived parameters are listed for the tubing vials (5800, 5816, 5811). The parameters for the 5304 vials are derived from single vial studies with two "typical" vials since multivial results are not available. In general, K_v data from single vial studies are in satisfactory agreement with the correspondingly more accurate multivial data; the mean relative deviation in K_v is <6%. For the 5303 vials, the agreement between multivial and single vial data is less satisfactory, and this lack of agreement in K_v data is reflected in a comparison of the heat transfer parameters (K_c and l) obtained from the two data sets (Table VIII, footnote *c*). Moreover, the standard error in l derived from the multivial data is unusually large. Lacking a satisfactory explanation for these observations, the K_c and l parameters reported (Table VIII) for the 5303 vials represent means of the results of single vial- and multivial-derived parameters.

The values of l (Table VIII) correlate reasonably well with the l_{max} data from Table I, where l_{max} is the approximate maximum separation distance between the vial surface and a flat surface. Linear regression gives:

$$l = 0.023 + 0.273\, l_{max} \qquad \text{(Eq. 23)}$$

with a correlation coefficient of 0.958. The values of K_c might be expected to correlate with the ratio of the contact area to the total vial area, denoted f_c, where the contact area is calculated from the diameter and thickness of the contact print. As a rough approximation, $10^4K_c = 12f_c$, but the correlation coefficient is only 0.76.

The uncertainties given (Table VIII) are standard errors provided by the computer output and are a useful indication of uncertainty only when data in Table VIII are compared. The value of K_c is particularly sensitive to changes in a_c and may also depend on the mathematical form chosen for K_g. An increase of 0.05 in a_c results in a decrease in 10^4K_c of 0.20. With the mathematical form of K_g fixed by Eq. 10, the standard error in a_c is ± ~0.05, corresponding to an absolute uncertainty in 10^4K_c of ±0.2. Note, however, that if the value of a_c is really 0.72 instead of 0.67, all values of 10^4K_c in Table VIII decrease by 0.2. The mathematical form of K_g (Eq. 10) is derived for two surfaces separated by a constant distance, l. The separation distance between the vial and the shelf is not a constant, but generally decreases as the radial distance from the center of the vial increases, until the contact print region is reached. As the radial distance increases further, the separation distance

Table X—Variation in Vial Heat Transfer Coefficients: Components of $\sigma(K_v)$ Defined by Eq. 25

Vial	RSD	
	Constant Term, $\sigma(K_K)$	Separation Distance, $\sigma(l)$
W5800	5.0	8.9
K5800	8.8	14.4
W5811	6.7	5.5
W5816	7.9	3.6
K5816	8.9	13.8
5303	4.6	7.0

increases sharply up to a maximum value characteristic of the vial. An alternate mathematical model for K_g (denoted model II), based on the vial bottom geometry discussed above, produces an extremely complex mathematical form for K_g[22]. Regression analysis of single vial and multivial data using K_g from model II yields an accommodation coefficient of 0.84 ± 0.04 and gives contact parameters, 10^4K_c, which are in good agreement with the corresponding parameters given in Table VIII. The quality of the fit is the same as that found using Eq. 10 for K_g. The absolute value of the difference between the corresponding values of 10^4K_c averages 0.14, as the parameters from model II are systematically lower. Thus, it appears that as long as the form of K_g provides a good fit to the data, the values of the contact parameter obtained are not extremely sensitive to the precise form of K_g used. We conclude that the systematic error in 10^4K_c introduced by the combination of uncertainty in a_c and uncertainty in the form of K_g is > ± ~0.3.

The energy accommodation coefficient, a_c, measures the efficiency of energy transfer in a collision between a gas molecule and a surface. For an elastic collision no energy is transferred and $a_c = 0$, while for a perfect inelastic collision, the gas molecule "equilibrates" with the temperature of the surface and $a_c = 1$. Since both the vial and shelf surfaces are involved in energy transfer, the accommodation coefficient for vial heat transfer reflects an average accommodation coefficient for gas molecule collisions with the two surfaces. For freeze-drying, the gas is nearly pure water vapor (Table III), and the error in a_c introduced by assuming the vapor is 100% H_2O is negligible[23]. Thus, although the value of a_c determined from the data may depend slightly on the model chosen for K_g, 0.67 ± 0.05 for Eq. 10 *versus* 0.84 ± 0.04 for Model II, both models suggest incomplete energy transfer ($a_c < 1$) for the collision of a water molecule with one (or both) of the surfaces involved. Due to the difficulties in evaluating an accommodation coefficient from vial heat transfer data, the conclusion, $a_c < 1$, must be regarded as tentative. Unfortunately, the accommodation coefficient data in the literature (12), do not include data for water vapor or glass surfaces.

Theoretically, the accommodation coefficient could depend on the nature of the shelf surface; however, at least for the two surfaces investigated, polished stainless steel and black paint, the K_v data (Table V) suggest such a dependence is minimal. The increase in K_v obtained with a black painted shelf (experiment 7 *versus* experiment 5, Table V), $\Delta 10^4K_v = 0.57 \pm 0.14$, is fully consistent with the observed increase in shelf emissivity, $\Delta e_s = 0.67 \pm 0.10$.

The relative importance of the three heat transfer mechanisms (radiation, contact conduction, and gas conduction) are compared in Table IX. Although the contact contributions are somewhat uncertain due to the possible systematic errors in K_c discussed earlier, it does appear that all three heat transfer mechanisms can make significant contributions to the total heat flow in freeze-drying. The dominant mechanism depends on both the chamber pressure and the type of vial considered. At chamber pressures >0.1 mm Hg, the dominant mechanism is gas conduction, but even at 0.4 mm Hg, both radiation and contact conduction can be important for some vials.

[22] Model II assumes that the vial bottom curvature near the shoulder is described by a semicircle of radius k_s while the curvature in the middle of the vial may be approximated by the arc of a circle. The arc and semicircle meet at $r = a$ (near the contact print region). Thus, K_g is obtained by integration of Eq. 10 over the radial distance $0 \le r \le r_v$, where r_v is the vial radius, $\sqrt{A_v/\pi}$, and the separation distance, l, is a function of r. For $0 \le r \le a$, the equation for an arc is used to obtain $l(r)$, while for $a \le r \le r_v$, the equation of a semicircle is used to evaluate $l(r)$. The value of a is calculated from $r_v = a + k_s$, where k_s is measured from the vial geometry and found to be 0.25 cm (10-mL vials), 0.32 cm (20-mL vials), and 0.44 cm (5303 vials). The resulting expression for K_g may be written in the form: $K_g = [(\lambda_0/h)/(1 + k_s/a)^2] \cdot \ln [1 + (\Lambda_0/\lambda_0)\alpha hP] + [2(ks/a)\Lambda_0\alpha P/(1 + ks/a)^2] \int_0^1 [1 + (ks/a)x]dx/[1 + (ks\Lambda_0\alpha P/\lambda_0)(1 - \sqrt{1 - x^2})]$ where h is the distance between the shelf and the vial bottom at the vial center (r = 0), and x is a dummy variable. The remaining symbols are as previously defined. The definite integral is a function of pressure, P, which must be evaluated by numerical procedures. Regression analysis of the data using the model II function for K_g gives an excellent fit to the data, but the values of h determined from the regression analysis are consistently a factor of ~2 larger than the measured separation distances (Table I).

[23] The average mole fraction of air (Table III) is ~0.15. Assuming that the value of Λ_0 is a weighted average of the Λ_0 data for water vapor and air, with the mole fraction of each component as the corresponding weight, the value of Λ_0 is calculated as 5.98×10^{-3} (P in mm Hg), compared with 6.34×10^{-3} for pure H_2O. Using 5.98×10^{-3} for Λ_0 increases the value of a_c determined from the data by only 0.03.

Table XI—Variation in Sublimation Rate Attributable to Tube Variation

Tube/Vial	Percent Deviation from Run Mean M	46	60	47	41	Row Mean
1	−0.17	−3.40	−5.42	−4.26	−5.06	−3.66
2	2.66	−4.97	−5.73	−4.63	−4.42	−3.44
3	2.14	−3.94	−5.70	−5.11	−3.92	−3.35
4	0.79	−3.93	−6.40	−5.64	−4.88	−4.01
5	−2.60	−3.42	−5.98	−4.84	−6.38	−4.64
Column Mean	0.56	−3.93	−5.91	−4.90	−4.93	−3.82

Analysis of Variance

Component	Variance, %²
Total, $\hat{\sigma}^2(\dot{m})$	6.42
Column Average (vial), $\hat{\sigma}_{\bar{c}}^2$	6.49
Row Average (tube), $\hat{\sigma}_{\bar{R}}^2$	0.27
Measurement Error, σ^2	1.18[a]
Column Effect (σ_c^2), σ_c^2	6.25
Row effect (tube), σ_R^2	0.03[a]

[a] Excluding M vial: $\sigma^2 = 0.44$, $\sigma_R^2 = 0.05$.

The pressure dependence of K_v is illustrated in Fig. 7 for several vials. The data shown are evaluated from the parameters in Table VIII. The curvature is a reflection of the importance of the separation distance, l, which is highly vial specific. Thus, particularly at high pressure, the vial heat transfer coefficient is quite sensitive to the geometry of the vial bottom.

Intervial Variability in K_v*: Pressure Dependence*—While there is no obvious pressure dependence in the $\sigma(K_v)$ data, theoretical considerations suggest a small but significant pressure dependence may be obscured by the lack of precision in the data. Assuming the variation in K_v arises from both variation in the pressure-independent term, $K_r + K_c$, and from variation in the separation distance, l, the variance in K_v is written:

$$\sigma^2(K_v) = \left(\frac{\partial \ln K_v}{\partial \ln K_K}\right)^2 \cdot \sigma^2(K_K) + \left(\frac{\partial \ln K_v}{\partial \ln l}\right)^2 \cdot \sigma^2(l) \qquad \text{(Eq. 24)}$$

where K_K denotes the pressure independent part of K_v, $K_K = K_r + K_c$, and the sigmas represent *RSD* values. Equation 24 also assumes that the deviations in K_K and l are not correlated. Evaluation of the derivatives in Eq. 24 then gives:

$$\sigma^2(K_v) = \sigma^2(K_K)G1(P) + \sigma^2(l)G2(P) \qquad \text{(Eq. 25)}$$

where $G1$ and $G2$ are functions of pressure:

$$G1(P) = (1 + k_D \cdot P)^2/[1 + (k_D + k_p/k_K)P]^2 \qquad \text{(Eq. 26)}$$

$$G2(P) = (k_p/k_K)^2 \left[\frac{k_p \cdot P^2}{1 + k_D P}\right]^2/[1 + (k_D + k_p/k_K)P]^2 \qquad \text{(Eq. 27)}$$

where $k_D = (\Lambda_0/\lambda_0)\alpha \cdot l$, $k_p = \Lambda_0\alpha$, and the other symbols have their usual meanings. The functions, $G1$ and $G2$, depend on vial type as well as pressure, but at low pressure $G1 \gg G2$, and at 0.4 mm Hg, $G2$ is slightly larger than $G1$.

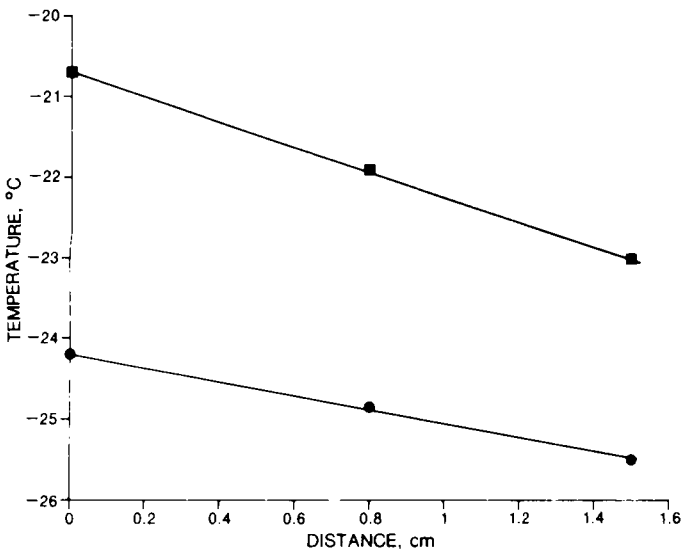

Figure 9—*Product temperature as a function of distance from the vial bottom. Key: (●) heat flux = 5.4 mcal/cm²·s, (■) heat flux = 10.6 mcal/cm²·s.*

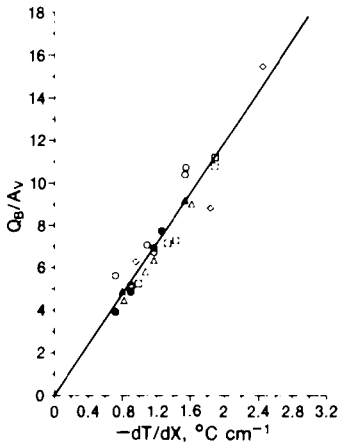

Figure 10—*Heat flux as a function of temperature gradient in the frozen product;* $\dot{Q}_B = \Lambda_r K_I[-dT/dx]$*;* $10^3 K_I = 5.9 \pm 0.4$*. Key: (○) W5800, (●) W5800 (5% KCl), (□) K5800, (△) W5811, (◇) W5816.*

Formally, Eq. 25 gives $\sigma^2(K_v)$ as a function of two variables, $G1$ and $G2$, with $\sigma(K_K)$ and $\sigma(l)$ as parameters. Regression analysis of the $\sigma(K_v)$ data, according to Eq. 25, produces "experimental" values for $\sigma(K_K)$ and $\sigma(l)$ (Table X). Presumably, variation in the contact term is the major contributor to $\sigma(K_K)$. The data are well represented by Eq. 25, but neither the precision nor the extent of the data is sufficient to establish the validity of Eqs. 25–27. Rather, provided one assumes the theoretical analysis in Eqs. 25–27 is valid, the data are sufficient to establish both $\sigma(K_K)$ and $\sigma(l)$ for each vial type with slightly better accuracy than the accuracy in the input $\sigma(K_v)$ data. The means of $\sigma(K_K)$ and $\sigma(l)$ for all W tubing vials are 6.5 and 6.0, respectively; the corresponding means for K tubing vials are 8.8 and 14.1, respectively. Thus, the K vials display somewhat greater relative variability, particularly in the separation distance. Calculated values of $\sigma(K_v)$, Eq. 25, for the average W and average K vials do show a pressure dependence (Fig. 8), the variability in K_v passing through a minimum at ~0.15 mm Hg. Particularly with K tubing vials where the minimum is relatively pronounced, primary drying will be more uniform if the chamber pressure is maintained between 0.1 and 0.2 mm Hg.

Intravial Temperature Distribution—The temperature of the frozen mass in the vial is routinely measured at four locations (Fig. 1) during all single vial experiments. No significant temperature difference is observed between the bottom center and bottom edge of the vial, suggesting that radial heat flow is minimal. As expected, however, the temperature decreases linearity with distance, X, from the vial bottom (Fig. 9), the slope increasing in magnitude as the heat flow through the bottom of the vial increases. Theoretically, the heat flow rate through the bottom of the vial, $\dot{Q}_B$, should be directly proportional to the temperature gradient, $\partial T/\partial X$ (Eq. 15). Evaluating $\dot{Q}_B$ as previously described yields the data shown in Fig. 10. Within the precision in the data, the heat flux, $\dot{Q}_B/A_v$, is directly proportional to the measured temperature gradient. The scatter in the data is largely a consequence of the uncertainty in temperature measurement. The slope appears to be independent of vial type; moreover, the data for KCl solutions do not deviate significantly from the data obtained using pure water. It appears that, independent of the vial type or product, the temperature distribution in a vial may be characterized by Eq. 15 with a constant value for the effective product thermal conductivity, K_I. Regression analysis yields $10^3 K_I = 5.9 \pm 0.4$. Theoretically, K_I contains contributions from both the frozen mass and the glass, Eq. 16. From the vial dimensions (Table I) and the thermal conductivity of glass (13), the thermal conductivity of the frozen product, κ_p, is calculated: $10^3\kappa_p = 6.6 \pm 0.5$ cal/s-cm-°C, in excellent agreement with literature data for ice (6, 7) at corresponding temperatures (−25°C).

CONCLUSIONS

The vial is an extremely important variable in the primary-drying stage of the freeze-drying process. Although the direct effect of the vial on mass transfer (*via* closure resistance) is slight, the nature of the vial does significantly affect the rate of heat transfer to the product and is a major factor in determining the product temperature and drying time for a given set of chamber pressure–shelf temperature settings. Vial heat transfer coefficients increase with increasing chamber pressure, but the pressure dependence is nonlinear. At high pressures, the coefficients are less sensitive to changes in pressure. The magnitude of the vial heat transfer coefficient is sensitive to the geometry of the vial bottom. While the thickness of the glass in the vial bottom

Table XII—Variation in Sublimation Rate Attributable to Vial Position

Position/ Vial[a]	Percent Deviation from Run Mean 24	16	48	59	7	Row Mean
1	−4.12	−5.87	−2.41	−3.13	−2.74	−3.65
2	−5.64	−5.46	−0.56	−4.86	−4.69	−4.24
3	−2.22	−4.49	3.77	−4.58	−3.73	−2.25
4	4.56	−1.48	3.30	−0.72	2.25	1.58
5	−3.18	−3.66	−1.62	−6.08	−5.06	−3.92
Column Mean	−2.12	−4.19	0.50	−3.87	−2.79	−2.50

Analysis of Variance

Component	Variance Including Position 4	Excluding Position 4
Total, $\hat{\sigma}^2(\dot{m})$	9.52	5.14
Column Mean, $\hat{\sigma}_{\bar{C}}^2$	3.49	3.62
Row Mean, $\hat{\sigma}_{\bar{R}}^2$	5.77	0.77
Measurement Error, σ^2	2.70	1.48
Column Effect (σ_v^2), σ_c^2	2.95	3.25
Row Effect (Position), σ_R^2	5.23	0.47

[a] Position 4 is class A (adjacent to shelf temperature sensor); all others are class H.

is not important, both the average separation distance between the vial bottom and the shelf and the degree of physical contact between the vial and the shelf are critical factors. The *RSD* in vial heat transfer coefficients, reflecting variability within a given lot of vials, is rather small (≈4%). However, large differences in vial heat-transfer coefficients exists between different types of vials. Even vials of nominally the same specifications, manufactured by different suppliers, differ significantly in their heat transfer characteristics. A freeze-drying cycle, optimized using one type of vial, cannot be expected to perform satisfactorily with a different vial. Indeed, circumstances may arise where a product is routinely freeze-dried with excellent yield, but a change of supplier for vial stock results in significant product loss arising from eutectic melt. Clearly, heat transfer characteristics must be given serious consideration when vial specifications are determined.

APPENDIX I: Data Analysis for K_v and $\sigma(K_v)$ Evaluation

Evaluation of Intervial Variability $\sigma(K_v)$—The multivial experiment directly yields the estimated variance in the sublimation rate for a given set of vials, $\hat{\sigma}^2(\dot{m})$. The desired parameter is the *RSD* in the vial heat transfer coefficients, $\sigma(K_v)$, and considerable data reduction is needed to extract $\sigma(K_v)$ from the raw data. First, components of variance in $\dot{m}$, due to causes unrelated to the vial heat transfer coefficient, must be subtracted from the estimated variance in $\dot{m}$, $\hat{\sigma}^2(\dot{m})$, to obtain the variance in $\dot{m}$ due to variation in the vials, σ_v^2. Second, the calculated value of σ_v must be converted into the corresponding value of $\sigma(K_v)$.

In addition to variation in vial heat transfer coefficients, three sources of variation in sublimation rate are possible: (*a*) variation in the mass transfer coefficients of the metal tubes, (*b*) variations due to location of the vial on the shelf originating from variations in shelf surface temperature and variations in radiation effects, and (*c*), measurement error or intrinsic variation in the procedure itself, probably resulting mostly from variability in the surface area and contour of the ice-vapor interface[24].

A series of six multivial experiments at a chamber pressure of 0.2 mm Hg were designed to evaluate the various components of variance in sublimation rate. The entire series of experiments were carried out with the same set of W5800 vials in the laboratory dryer. For most of the vials, the vial number, the metal tube used, and the shelf position were held constant throughout the series to allow evaluation of the intrinsic variation or "error" component of the variance, σ^2. For the first five experiments, a subgroup of five vials and corresponding positions were fixed, and the five metal tubes were rotated among the subgroup to determine the effect of variation in metal tube on the sublimation rate. A second subgroup of five vials, with corresponding metal tubes, were rotated among five selected shelf positions to determine the effect of shelf positions on the sublimation rate. The vial placement used in these studies is shown in Fig. 5, where each vial is shown as a circle. The term "pressure tube channel" denotes the space occupied by the tube connecting

[24] Particularly with pure ice, the ice-vapor interface does not remain perfectly planar during the entire experiment. While the mass transfer resistance of the solid to vapor phase transition is small, it is not zero (3), and variation in surface area will therefore have a small effect on the overall mass transfer resistance. Moreover, the effective thickness of the ice plug for heat transmission from the vial bottom may vary slightly between vials or between replicate experiments with the same vial. Thus, even for fixed K_v and fixed T_s, the sublimation rate will vary slightly within a given set of vials.

Table XIII—Sublimation Rate Variation in Pilot Dryer: Percent Deviation from Mean Sublimation Rate Related to Vial Position[a]

Row/ Column	Percent Deviation from Run Mean 1	2	3	4	5	Row Mean, $\bar{R}_i$
1	−4.17	−4.64	−4.47	−3.60	1.79	−3.02
2	−3.47	−7.14	−1.85	−3.75	0.41	−3.16
3	−2.21	−3.52	−4.79	−4.78	0.15	−3.03
4	−1.59	0.14	−7.20	1.08	1.20	−1.27
5	−6.61	1.85	1.26	−0.79	2.46	−0.37
6	−0.28	3.48	5.48	5.51	−1.74	2.49
7	5.66	1.29	4.71	3.75	3.34	3.75
8	−1.22	1.74	3.15	5.22	13.58	4.49
9	1.16	1.31	2.55	2.13	6.55	2.74
10	−4.28	−3.91	0.00	−0.50	4.04	−0.93
11	−0.14	−5.12	−2.26	−3.96	3.23	−1.65
Column Average, $\bar{C}j$	−1.56	−1.32	−0.31	0.03	3.18	0.00

Analysis of Variance

Component	Variance
Total, $\hat{\sigma}^2(\dot{m})$	16.28
Column Average, $\hat{\sigma}_{\bar{C}}^2$	3.60
Row Average, $\hat{\sigma}_{\bar{R}}^2$	8.16
Measurement Error, σ^2	1.99
Column Effects, σ_c^2	3.41
Row Effects, σ_R^2	7.76
Vial, σ_v^2	5.83

[a] 5303 vials, 0.2 mm Hg.

the interior of the modified vial to the pressure sensor. Vials on the edge of the shelf, which are exposed to the chamber walls, are marked with an E. All other (interior) vials are divided into two classes: class A, which represents those vials adjacent to a shelf temperature sensor, and class H, where the vial is in a hexagonal close-packed configuration with other vials, as would be found in normal loading of a freeze-dryer. Vials adjacent to the pressure tube channel are not rigorously in a hexagonal configuration, but the results of this series of experiments and subsequent multivial experiments indicate that vials adjacent to the pressure tube channel show no measureable position bias when compared with hexagonally packed vials. The vial identification number is given in the lower part of the circle, and the class A vials have a bar underlining the vial number. [The modified vial (Fig. 1) is denoted M.] The symbols P_1, P_2, P_3, P_4, and P_5, refer to the positions used in the position rotation study while the symbols T_1, T_2, . . . , refer to vials-positions used in the tube rotation study. Thermocouple-containing vials have the designation TC, followed by the thermocouple identification numbers, or numbers in the case of multiple-thermocouple vials. The number in the top part of the circle, containing a decimal point, is the percent deviation of the mean sublimation rate for that vial-position combination from the corresponding mean for the total interior set of vials. The deviations recorded for the P vials correspond to the mean deviation for that position as found in the position rotation study.

The edge vial deviations represent the results of a single experiment but clearly show a higher sublimation rate than the interior vials. The mean deviation in sublimation rate for the edge vials is 15.0 ± 1.5%, where the uncertainty is the *SD* of the mean. The higher sublimation rate for edge vials is undoubtedly due to radiation effects from the edge of the shelf and chamber wall. Since edge vials are atypical, edge vial data are excluded from the data analysis. It should also be noted that vial 22 (Fig. 5, upper left corner) behaves anomalously. The edge vials surrounding vial 22 displayed a tendency to move away from it during the course of the experiment, presumably due to vibrations, giving vial 22 some characteristics of an edge vial. Thus, vial 22 is also excluded from data analysis.

The raw data and corresponding analysis of variance for the metal tube rotation portion of the experiment (Table XI) show essentially zero variance in sublimation rate caused by variation in the mass transfer coefficient of the metal tubes. All standard deviations (σ) are relative standard deviations. The estimated or directly measured *SD* in the first three rows of the analysis of variance section are evaluated with $N - 1$ weighting from the raw data. The value of $\hat{\sigma}_{\bar{C}}$ is computed from the column means while the value of $\hat{\sigma}_{\bar{R}}$ is computed from the row means. The last three rows in the analysis of variance section are calculated variances for an infinite set of vials evaluated from the variances in the first three rows using the appropriate corrections for degrees of freedom (14). The measurement error component, σ^2, represents the intrinsic variability in the experiment while the column effect, σ_c^2, gives the variance originating from vial-position variability. The variance component giving the row effect, σ_R^2, represents the contributions to the variance in sublimation rate originating from variation in metal tubes. Clearly, variation in the mass-transfer coefficient of the metal tubes is negligible.

The results of the position rotation experiment (Table XII) indicate a significant position effect, but nearly all of this effect is due to a difference between class A and class H interior shelf positions. Indeed, when position 4 (class A) is excluded from the analysis, the remaining four positions yield a position variance of only 0.47. Thus, the shelf temperature uniformity appears to be excellent.

The mean bias between position 4 and the other positions is 5.1 ± 1.0%, where the uncertainty is the standard error in the bias estimate. Additional multivial experiments comparing class A positions with class H positions yield a bias of 3.6 ± 1.0%, in reasonable agreement with the value obtained from the data in Table XII. The higher sublimation rate for vials adjacent to a shelf sensor is probably a result of radiative heat transfer from the shelf sensor, at roughly the shelf temperature, to the vial. We write[25]:

$$\Delta\dot{Q}_A \cong A_v S_a \times 10^{-4} (T_s - T_b) \qquad \text{(Eq. 28)}$$

where $\Delta\dot{Q}_A$ is the extra heat flow coming from the shelf sensor. The parameter, S_a, evaluated from the data is 0.31.

The measurement error variance, σ^2, is estimated from the replication data for those vials where the vial position is held fixed for the series of six experiments. Using $N - 1$ weighting, the estimated variance is calculated for each vial, and the mean variance of each vial class is taken as the measurement error variance for that class. For class A vials $\sigma^2 = 4.3$, while for class H vials, $\sigma^2 = 2.6$.

For a set of N vials of which A vials are adjacent to a shelf temperature sensor, the total estimated variance in $\dot{m}$, $\hat{\sigma}^2(\dot{m})$, where $\hat{\sigma}(\dot{m})$ is the estimated *RSD* in $\dot{m}$, with $N - 1$ weighting, may be approximated by:

$$\hat{\sigma}^2(\dot{m}) = \sigma_v^2 + \sigma_{SP}^2 + (A/N)\sigma_{EA}^2 + (1 - A/N)\sigma_{EH}^2 + (A/N)(1 - A/N)r^2 \qquad \text{(Eq. 29)}$$

here, σ_v^2 is the variance component from variation in the vial heat transfer coefficient, σ_{SP}^2 is the variance component from shelf position variation for class H vials [0.47 (Table XII)], σ_{EA}^2 and σ_{EH}^2 are the measurement error components for class A (4.3) and class H (2.6) vials, respectively. The term in r gives the variance component originating in the class bias between class A and class H vials where:

$$r = 10^2 \frac{\Delta\dot{m}_A}{\langle\dot{m}\rangle} = \frac{0.0545\, A_v S_a (T_s - T_b)}{\langle\dot{m}\rangle} \qquad \text{(Eq. 30)}$$

The term, $\Delta\dot{m}_A$, is the difference in sublimation rate (g/h) between a class A vial and the mean sublimation rate for the entire set, $\langle\dot{m}\rangle$. From the variance data obtained in the series of preliminary experiments described in Tables XI, XII and Fig. 5, and the experimental value of $\hat{\sigma}^2(\dot{m})$ obtained for a given experiment, the corresponding variance due to variation in the vial transfer coefficient, σ_v^2, may be calculated. When A/N is ~0.5, the position bias term in Eq. 29 is large and may be the largest component of variance, thus limiting the accuracy with which σ_v^2 may be determined.

Equation 29 is an approximation where the most serious problem arises from the assumption that the measurement error variances and class bias do not vary between experiments. Clearly, the accuracy in σ_v^2 would be greatly improved with an experimental design where A/N is zero without decreasing N significantly. Originally, we were concerned with potential shelf temperature variation with position and chose to employ two shelf sensors at central locations on the shelf (A/N is ~0.4). However, experience has shown that shelf temperature variation is not a problem with the laboratory dryer, and our current experiment design uses only one shelf sensor at an edge vial location and does not use the modified (M) vial. Thus, the pressure tube channel is filled with vials. The net result is that only one vial from a set of ~15 is adjacent to the shelf sensor, and this vial is excluded from the data analysis. Only vials in a truly hexagonal packing arrangement are used in the data analysis.

The *RSD* in sublimation rate is slightly smaller than the corresponding *RSD* in the vial heat transfer coefficient. The sublimation rate is proportional to the product of K_v and the temperature difference, $T_s - T_b$. A given positive deviation in K_v produces a corresponding increase in T_b, thereby decreasing slightly the temperature difference, $T_s - T_b$, resulting in a net relative increase in $\dot{m}$ smaller than the relative increase in K_v. The *RSD* in K_v, $\sigma(K_v)$, may be related to the *RSD* in $\dot{m}$, σ_v by:

$$\sigma(K_v) = \sigma_v \cdot \frac{d \ln K_v}{d \ln \dot{m}} \qquad \text{(Eq. 31)}$$

where:

$$\frac{d \ln K_v}{d \ln \dot{m}} \cong 1.2 + 400\, K_v \qquad \text{(Eq. 32)}$$

Since K_v is of the magnitude 5×10^{-4}, the value of $\sigma(K_v)$ is ~50% greater than σ_v. The derivation of Eq. 32 is given in *Appendix II*.

Due to significant shelf position effects, evidently originating, at least in part, from nonuniformity of shelf temperature, the statistical analysis for data generated with the pilot dryer differs slightly from the analysis (Eq. 29) given data from the laboratory dryer. The procedure used with data from the pilot dryer is outlined in Table XIII. Here, the rows and columns represent vial locations on the dryer shelf. The numbers within the row-column matrix are percent deviations of the sublimation rate for a given vial-position from the mean sublimation rate of all interior vials. The *RSD* ($\hat{\sigma}(\dot{m})$, $\hat{\sigma}_{\bar{c}}$, and $\hat{\sigma}_{\bar{R}}$) are evaluated directly from the raw data as described previously in the discussion of Table XI. The last four rows in the analysis of variance section of Table XIII are calculated data (14)[26] using $\sigma^2 = 1.99$. This value of σ^2 is determined from a series of replication experiments with 5303 vials in the pilot dryer. Note that the column position effect, σ_c^2, and row position effect, σ_R^2, are major contributors to the total variance. The term of interest, the variance in $\dot{m}$ due to vial heat transfer variations, σ_v^2, is <50% of the total variance.

Evaluation of Vial Heat Transfer Coefficients From Multivial Data—The vial heat transfer coefficient is formally defined by Eq. 8 when the surface above the vials is at the temperature of the shelf. For both the laboratory and pilot dryers, the temperature of the surface above the vials differs somewhat from the shelf temperature. Moreover, although the average sublimation rate is measured, from which the mean heat transfer rate may be calculated, the temperature difference $T_s - T_b$ is measured for a limited number of vials, normally four. Therefore, the average temperature difference corresponding to the average heat-transfer rate is not directly measurable, and an indirect calculation procedure is used to evaluate the average heat transfer coefficient.

First, the mean heat transfer rate corresponding to heat flow through the vial bottom, $\langle\dot{Q}_B\rangle$, is evaluated from the mean heat transfer rate, $\langle\dot{Q}\rangle$, by subtraction of the top radiation contribution:

$$\langle\dot{Q}_B\rangle = \langle\dot{Q}\rangle - A_v e_v \sigma (T_L^4 - T^4) \qquad \text{(Eq. 33)}$$

where σ is the Stefan-Boltzmann constant, T_L is the temperature of the surface above the vials, and e_v is taken as 0.84 (Table IV). The value of $\langle\dot{Q}\rangle$ in cal/s is calculated from the mean sublimation rate in g/h by $\langle\dot{Q}\rangle = 0.1833\langle\dot{m}\rangle$. The temperature, T_L, is directly measured, and the temperature of subliming ice, T, is evaluated indirectly from the mean sublimation rate and the chamber pressure. Since the gas in the vial is essentially pure water vapor at the equilibrium vapor pressure of the subliming ice, the mean sublimation rate, mean vapor pressure, and chamber pressure are related (Appendix II, Eq. 41). Thus, the mean vapor pressure is determined from the mean sublimation rate, and the corresponding mean ice temperature, $\langle T\rangle$, is evaluated from the mean vapor pressure[15]. Equation 33 is used to evaluate the mean heat transfer rates for both the set of thermocouple-containing vials and the complete vial set.

That portion of the vial heat transfer coefficient representing heat transfer from the shelf to the vial bottom, denoted K_{vB}, is evaluated for the set of thermocouple-containing vials:

$$\langle K_{vB}\rangle_{TC} = \langle\dot{Q}\rangle_{TC}/A_v\langle T_s - T_b\rangle \qquad \text{(Eq. 34)}$$

where the subscript TC denotes the mean of the thermocouple vial set. The mean of K_{vB} for all vials, denoted $\langle K_{vB}\rangle$, is obtained indirectly. In general, the value of $\langle\dot{Q}_B\rangle_{TC}$ is slightly different from the corresponding mean of all the vials, $\langle\dot{Q}_B\rangle$. Treating this small difference as a differential, $d\langle\dot{Q}_B\rangle \cong \langle\dot{Q}_B\rangle - \langle\dot{Q}_B\rangle_{TC}$, the corresponding differential in $\langle K_{vB}\rangle$, $d\langle K_{vB}\rangle = \langle K_{vB}\rangle - \langle K_{vB}\rangle_{TC}$, may be evaluated from the value of the derivative, $d \ln K_{vB}/d \ln \dot{Q}_B$ (Appendix II, Eq. 45). Thus, the value of $\langle K_{vB}\rangle$ is given by:

$$\langle K_{vB}\rangle = \langle K_{vB}\rangle_{TC}\,[1 + (1.2 + 400\,\langle K_{vB}\rangle_{TC}) \cdot (\langle\dot{Q}_B\rangle/\langle\dot{Q}_B\rangle_{TC} - 1)] \qquad \text{(Eq. 35)}$$

The value of $\langle K_{vB}\rangle$ calculated from Eq. 35 refers to the mean of all vials and, therefore, includes the effects of atypical radiation heat transfer from the shelf sensor for the class A vials. The result of Eq. 35 is corrected to represent only class H (normal position) vials by subtracting the term, $S_a \times 10^{-4}\,(A/N)$, (see Eq. 28) from $\langle K_{vB}\rangle$. Finally, the total vial heat transfer coefficient, as defined by Eq. 8, is obtained by adding $e_v \times 10^{-4}$ to the corrected result from

[25] Heat flow from the shelf sensor to the vial is probably proportional to the "cylinder" area of the vial, A_c. However, for the vials studied, A_c is approximately proportional to the cross-sectional vial area, A_v.

[26] For a matrix of deviations containing p rows and q columns, where the rows and columns represent position effects, the random component of variance is the sum, $\sigma_v^2 + \sigma^2$, which may be evaluated from (14): $\sigma_v^2 + \sigma^2 = [(pq - 1)/(p - 1)(q - 1)]\hat{\sigma}^2(\dot{m}) - p/(p - 1)\hat{\sigma}_{\bar{c}}^2 - [q/(q - 1)]\,\hat{\sigma}_{\bar{R}}^2$.

Eq. 35 to provide for the correct top radiation term under the conditions of Eq. 8. Thus, the mean value of K_v for the vial set is:

$$K_v = \langle K_{vB} \rangle - S_a \times 10^{-4} (A/N) + e_v \times 10^{-4} \qquad \text{(Eq. 36)}$$

where $\langle K_{vB} \rangle$ is given by Eq. 35, S_a is taken as 0.31, and e_v is 0.84 (Table IV).

APPENDIX II: Relationship of Relative Standard Deviation in K_v with Relative Standard Deviation in $\dot{m}$

The relationship of $\sigma(K_v)$ to $\hat{\sigma}(\dot{m})$ depends on the derivative, $d\ln K_v/d\ln \dot{m}$ according to Eq. 31. This derivative may be evaluated with sufficient accuracy assuming the temperature of the source of top radiation is equal to the shelf temperature, T_s. With this assumption, the sublimation rate, $\dot{m}$ (g/h) may be written:

$$\dot{m} = \frac{3600\, A_v K_v}{\Delta \overline{H}_s} (T_s - T_b) \qquad \text{(Eq. 37)}$$

where $\Delta \overline{H}_s$ is the heat of sublimation and the factor, 3600, converts sublimation rate from g/s to g/h. Similarly, the sublimation rate may be related to the temperature difference between the bottom of the vial and the temperature of subliming ice using the approximation:

$$\dot{m} \cong \frac{3600\, A_v K_I}{\Delta \overline{H}_s} \frac{(T_b - T)}{l_i} \qquad \text{(Eq. 38)}$$

where l_i is the thickness of the ice plug and T is the temperature of the subliming ice. The relationship given by Eq. 38 is rigorous only when all heat flow comes through the vial bottom. However, the error introduced by using Eq. 38 does not seriously affect the results of this section. Differentiation of Eq. 37 yields:

$$\frac{d \ln K_v}{d \ln \dot{m}} = 1 + 3600 \frac{A_v K_v}{\Delta \overline{H}_s} \left(\frac{d\dot{m}}{dT} \cdot \frac{dT}{dT_b} \right)^{-1} \qquad \text{(Eq. 39)}$$

while differentiation of Eq. 38 gives:

$$\left[\frac{dT}{dT_b} \right]^{-1} = 1 + \left(\frac{l_i \Delta \overline{H}_s}{3600 A_v K_I} \right) \cdot \frac{d\dot{m}}{dT} \qquad \text{(Eq. 40)}$$

The sublimation rate may also be related to the pressure in the vial using Eqs. 3, 7, and 17. Since in multivial experiments with pure water, the pressure in the vial is approximately equal to the equilibrium vapor pressure of ice (P_0), one may write:

$$\dot{m} = a_0 (P_0 - P_c) + \frac{a_1}{2} (P_0^2 - P_c^2) \qquad \text{(Eq. 41)}$$

with $a_0 = 0.2478$ and $a_1 = 1.944$. Thus, since $d\dot{m}/dT = (d\dot{m}/dP_0)(dP_0/dT)$:

$$\frac{d\dot{m}}{dT} = (0.2478 + 1.944\, P_0) \frac{dP_0}{dT} \qquad \text{(Eq. 42)}$$

Combining Eqs. 39-42 and using $dP_0/dT \approx 0.1\, P_0^{1.5}$:

$$\frac{d \ln K_v}{d \ln \dot{m}} = 1 + \frac{l_i}{K_I} K_v + \frac{3.6 \times 10^4 A_v K_v}{\Delta \overline{H}_s (0.2478 + 1.944 P_0) P_0} \qquad \text{(Eq. 43)}$$

Numerical evaluation of the term involving P_0 demonstrates that this term is nearly constant at 0.2 for all multivial experiments conducted. Thus, with $l_i \approx 2.3$ cm and $K_I = 5.9 \times 10^{-3}$ (Fig. 9), Eq. 43 simplifies to:

$$\frac{d \ln K_v}{d \ln \dot{m}} = 1.2 + 400\, K_v \qquad \text{(Eq. 44)}$$

A derivation nearly identical to that given above may be given to evaluate the derivative $d \ln K_{vB}/d \ln \dot{Q}_B$, where K_{vB} is that portion of the heat transfer coefficient describing heat transfer from the shelf to the vial bottom, and $\dot{Q}_B$ is the heat flow from the shelf to the vial bottom. The result is also nearly identical to Eq. 44 and may be written:

$$\frac{d \ln K_{vB}}{d \ln \dot{Q}_B} = 1.2 + 400\, K_{vB} \qquad \text{(Eq. 45)}$$

Equation 45 is used in the evaluation of vial heat transfer coefficients from the raw data.

REFERENCES

(1) T. A. Jennings, *Drug Cosmet. Ind.*, **127**, 43 (1980).

(2) A. P. MacKenzie, *Ann. N.Y. Acad. Sci.*, **125**, 522 (1965).

(3) M. J. Pikal, S. Shah, D. Senior, and J. E. Lang, *J. Pharm. Sci.*, **72**, 635 (1983).

(4) S. L. Nail, *J. Parenter. Drug Assoc.*, **34**, 358 (1980).

(5) S. Dushman and J. M. Lafferty. "Scientific Foundations of Vacuum Technique," 2nd ed., Wiley, New York, N.Y., 1962.

(6) R. W. Powell, *Adv. Phys.*, **7**, 235 (1958).

(7) T. Ashworth, Proceeding International Cryogenic Engineering Conference, 4th ed., IPC Sci. Technol. Press, Ltd., Guilford, Engl., 1972, p. 377.

(8) G. Janesco, J. Pupezin, and W. A. VanHook, *J. Phys. Chem.*, **74**, 2984 (1970).

(9) F. P. Incropera and D. P. DeWitt, "Fundamentals of Heat Transfer," Wiley, New York, N.Y., 1981.

(10) J. Amoignon, "Freeze Drying and Advanced Food Technology," Academic, London, 1975, p. 445.

(11) J. R. Partington, "An Advanced Treatise on Physical Chemistry," vol. 1, Wiley, New York, N.Y., 1949.

(12) F. O. Goodman and H. Y. Wachman, "Dynamics of Gas-Surface Scattering," Academic, New York, N.Y., 1976.

(13) "International Critical Tables," vol. 4, McGraw-Hill, New York, N.Y., 1929, p. 217.

(14) C. A. Bennett and N. L. Franklin, "Statistical Analysis in Chemistry and the Chemical Industry," Wiley, New York, N.Y., 1954.